Responses to reviewer comments on 'Photochemical impacts of haze pollution in an Urban Environment'.

The authors would like to thank both reviewers for their detailed and useful comments on our manuscript. Please find below our responses to each reviewers comment. The comment from the reviewer is shown in italic and our response is shown in bold. We also highlight changes in the revised manuscript in red. A tracked changes version of the manuscript is shown at the end of these responses.

Anonymous reviewer 1:

P1/Abstract. I urge you to drop the decimal place on these per cents. I For example, think that 40-60% adequately describes 40.4-66.2%. Also, I think that the key statement quoted above (P12/L20ff) should appear in the abstract. This is a powerful result and should be up front.

We thank the reviewer for this suggestion. We have removed the decimal place from the abstract for clarity, and have also amended this in other places in the paper. We have also added the following key statement to the end of the abstract:

'Idealised photochemical box model studies show that such large impacts on photochemistry could lead to a 12% reduction in surface O_3 (3% for OH) due to haze pollution. This therefore highlights that any $PM_{2.5}$ mitigation strategies could have important implications for the oxidation capacity of the atmosphere both at the surface and in the free troposphere.'

P2/L5 I would have expected the original 2 papers that calculated the aerosol photolytic effects to be noted here: Martin et al, and Bian et al., both 2003.

We agree that this was an oversight and have added the suggested references on the photolytic effects of aerosols.

P3/L12 Curious. Why in 'North' capitalized here? in US English, I would think not.

We thank the reviewer for spotting this error. North should not be capitalised here and has been corrected in the revised manuscript.

P4/L1 I read through the Whalley 2018 paper and looked up their supplemental data and cannot find any source of cross section data for photolysis. Is this the correct source?

This method used to determine measured photolysis rates in the Beijing campaigns was the same as used in the ClearFlo project described by Whalley et al 2018 hence why we have cited this paper here. The sources of the cross sections and quantum yields are IUPAC and JPL.

P4/L13 does non-refractory aerosol include semi or partly volatile SOA?

The Aerosol mass spectroscopy (AMS) data only provided speciation of aerosol to sulphate, nitrate chloride and lumped organic aerosol. The lumped organic component will contain semi volatile SOA. This has been explored through PMF analysis in other parts of the APHH Beijing Programme however for the purposes of this study we have used the lumped OA in the Fast-JX simulations.

P4/L31 Eqn I am trying to understand the units here. b (extinction) should be in 1/Mm, right? But [X] is usually a concentration unit (#/cm3). So please assign units carefully to all to help this reader.

We apologise for the confusion here. As described in the original paper defining the IMPROVE algorithm for attributing extinction to aerosol species (Pitchford et al., 2007) the coefficients in equation 1 are the mass scattering/absorption efficiency (MSE/MAE) for each aerosol species. These have units of m^2/g. In our case our aerosol are specified as mass concentrations ($\mu g/m^3$) and therefore will return units of inverse megametres (Mm^{-1}) for the extinction. We have clarified this in the revised manuscript.

P5/L3-12 Very nice design. I like the careful merger to get consistent measurement data for the modeling.

Thanks very much.

P5/L19 'account for' does not make sense to me, do you mean "average over" ?

This sentence was intended to indicate that in order to account for multiple layers of overlapping cloud in the atmospheric column we use a quadrature approach to average over cloud fractions in all layers. On the reviewers' suggestion we have changed 'account for' to 'average over' in the revised manuscript.

Can you specify what options/versions you used in Cloud-J, IF you implemented observed cloud fraction? Cloud fraction is not mentioned here, so make it clear that you just used a single column atmosphere, full cloud or clear in each layer.

We implemented the quadrature approach (Neu et al 2007, Prather et al 2015) for cloud cover here using to account for overlapping cloud layers in the column. The cloud cover fraction product from the ERA5 (with cloud fractions specified for each model layer) reanalysis product was used to implement cloud cover in FJX. We have clarified this in the revised manuscript.

P5/L21-33 This is a nice augment to the Fast-J code, both the NO2 absorption and the aerosol cross sections. Are they available as a mod to a Fast-J/Cloud-J version? They ought to be. Using H-G and asymmetry parameter is OK for generating the phase function, but Mie would be better (outside the scope of this paper I know).

The modifications made for the NO_2 absorption are not currently available as a mod to Fast-J/Cloud-J but we agree that they could be implemented into future versions of the code. The Mie approach would provide a more accurate method for generating the phase function but we have chosen a simpler approach for these studies at the present time due to the Mie approach being more computationally intensive.

P6/L8-27 The high-frequency comparison in Figure 1 is fascinating and it is interesting to see the mean bias over the diurnal cycle. Since you are using the same cross sections for both, it means that FJX is too hot, and overestimates the high-sun fluxes. Can you check if this holds for clear, unpolluted days?

FJX does appear to have a positive bias on both polluted and unpolluted days as shown in Figure 1. However, the availability of observed column ozone data was limited during both campaigns and therefore we used column ozone from the ERA5 reanalysis product. It is likely that the positive bias in FJX is related to biases in the ERA5 ozone column.

Also, I think it would be valuable here to add something like a correlation coefficient to test if FJX+'Observed aerosols' can match the daily variability. Just add the r2 to the right-hand figure.

We thank the reviewer for their suggestion. We have added correlation coefficients for both campaigns to the right hand figures in both plots in Figure 1 in the revised manuscript.

Use of %: Here is where the decimal point in the % numbers makes some sense (i.e., the bias). There are so many % numbers in this paper, it would be good to try to differentiate them simply. Otherwise the unit '%' should be fleshed out to say '% of what'. The % in a bias should maybe always have a sign: e.g., L13, +5.6 % mean bias above observations. See next section.

We thank the reviewer for the suggestion. This has been corrected in the revised manuscript.

P6/L32 Use of %: Maybe do not need % here, but always need units to be clear. "In winter (NH4)2SO4 (39% of all aerosols by mass? by number? by optical depth?) and BC (30%) provide: : :

We have corrected this in the revised manuscript and have clarified that the % values are the contribution to total column optical depth.

P7/L2 & Fig 2 "Vertical AOD profiles" and Fig 2 (bottom) make no sense in terms of units and what is plotted. The top row of Fig 2, it is the fraction of AOD from each component. Here the extra decimal point makes sense and does not clutter the reading. The problem is that AOD is always an extrinsic quantity while extinction (b, beta) is intrinsic. AOD is always integrated over a column or path length, but b is local. Thus you can plot b vs altitude, but not AOD. Please fix units in plot. See also L17 with "AOD values", and L20.

We apologise for the potential confusion in this plot. The top row in the figure is the fraction of total column aerosol apportioned to each species. For improved clarity we have replaced the pie charts with bar charts and included the numbers in the main manuscript text. The lower plots show the integrated AOD over each 30m layer in the lidar profile however can appreciate the confusion with the units in the plot. For clarity we have replaced the lower plots with those that show extinction (b_{ext}) vs altitude. The units of extinction will be inverse megametres (Mm^{-1}). We have edited the text in the revised manuscript to reflect this updated figure.

P7/L9 Use of %: here and elsewhere in this discussion, please round off. 20% is just fine instead of 19.8%, since the uncertainty is certainly greater than +-1%.

We have corrected this here and throughout the discussion. All % changes have been rounded to the nearest whole number.

P7/L27 Use of % again: We have 23.8 and 23.1% reductions, the extra decimal is not meaningful in this discussion. Also the units are not clear. J's are about -23 % below what? a clear sky? a sky with all the other pollution but only those removed? If the latter, it does raise the question of linearity or interference across the aerosol mix. All throughout this discussion the nearest % is more than adequate.

All % changes have been rounded to the nearest % in this section. The impacts of each individual aerosol species have been calculated by including each species in isolation and comparing the changes in J rates to those simulated under clear sky conditions. Therefore the changes presented

are the simulated effects from that particular species only. In the revised manuscript we clarify this by editing the first sentence of section 3.3 to read:

'As Fast-JX is run in offline mode, the effects of each aerosol species can be determined independently. Each aerosol species is allowed to influence incoming solar radiation in isolation (Table 1) allowing the change in photolysis rates with respect to clear sky conditions to be quantified (Figure 3). This allows quantification of the impacts of each species on photolysis rates during haze episodes in Beijing.'

P8L16 & Fig 4. I wonder if this figure should show absolute changes in J's instead of %. I would think that this would emphasize the reactivity better, since % changes at low sun are not really important. For something like J-HONO, this would be fine, since the J's are more of a square wave. Figures 3 & 5 are fine as is, even if you change this to absolute deltas. If you want, you could do % of some noontime mean.

We agree that % changes at low sun are of relatively low importance. We will change this figure to reflect absolute changes in J rates for both O_3 and NO_2 which will highlight the larger impacts during the middle of the data when photochemical activity is at its greatest.

P8L30-35 Yes, this is an important result. Aerosol-pollution scattering and absorption above the boundary layer could be the most important factor.

Thanks very much.

P9/L5+ You can note here that – as you have found for polluted boundary layer – clouds have a much greater relative impact on J[NO2] vs J[O1D] also in observations over the clean remote Pacific [Hall et al., acp-18-16809-2018, very new paper, also using FJX, not available at time of drafting this paper.]

We agree that our findings are consistent with that of Hall et al and have added the suggested reference to the revised manuscript.

P9/L11-17 I found this paragraph confusing, and could not get the message.

This paragraph aims to highlight that in haze events during the summer campaign clouds had a dominant effect on J-rates at the surface but that aerosols became increasingly important higher up the column. We have clarified this as follows in the revised manuscript.

"In summer, during haze conditions, clouds produce the largest impacts on photolysis rates in the surface layer (reductions of 10–11%), approximately double that attributed to aerosol (~6%). The effects of high levels of scattering aerosol (particularly OA) during these conditions are evident higher in the column where increases in photolysis rates due to aerosol are much larger than those from clouds. The combined effects of cloud and aerosol are reductions in the lowest 3 km (0.1–17.2% for $J[O^1D]$ and 1.2–15.7% $J[NO_2]$) which are dominated by the influence of clouds. Between 3-6 km the effects of backscatter from aerosol are greater than those from clouds giving net increases in photolysis rates (8.8–13.7% for $J[O^1D]$ and 11–18% $J[NO_2]$)"

P9-P12 Discussion This section is long and to me it wanders. If this discussion is useful, please do some numbered sub-sectioning for the reader.

We thank the reviewer for this suggestion. We have edited the discussion slightly to tighten up the flow and readability of the discussion. This has been done by separating out the discussion on the

simple box model studies into its own sub-section at the end of the discussion section in the revised manuscript.

P10/L27 "would be balanced by : : : rise ion NO: : :" To me this is not logical, since more NO means that less of O3 is tied up as NO2 in the NOx emissions, and further, more NO would enhance the ROO+NO reactions? Does this not augment the enhanced production rates? as oppose to balance them?

The enhanced NO_2 photolysis would produce more NO which would subsequently react with O_3 to form NO_2. However the reviewer is correct in pointing out that added NO would also enhance ROO+NO reactions which would lead to higher O_3 concentrations. We have clarified this point in the revised manuscript to confirm the net increase in O_3 from this pathway.

'Enhanced near-surface photolysis rates would also increase O_3 production via NO_2 photolysis and enhanced levels of NO. This rise in O_3 will be partially balanced by the reaction of NO with O_3 itself. However, higher NO levels will also contribute to enhanced O_3 formation through increases in RO_2 and NO reactions. Furthermore, the enhancement of $J[O^1D]$ would increase OH concentrations which would subsequently increase HO_2 and RO_2 and lead to a net rise in O_3 concentrations.'

P11/L6 Use of %: "around 12.0%", really. "by 12 % and 3 %, respectively."

We have corrected this in the revised manuscript.

P13/L10 It seems that I have read something like this before. Do you need to repeat?

This sentence was to highlight the improvement this study makes on previous all modelling based studies as part of the paper conclusions. However we appreciate it is repetitive and have therefore tightened up this paragraph to read as follows.

"The observation-driven approach to deriving the aerosol vertical distribution allows a more accurate constraint to be made on the estimated impacts of haze pollution on photochemistry and, more critically, allows species specific impacts to be highlighted. This allows the potential identification of source sectors to target particulate control strategies on. "

P13/L27 I think you need to have both observational data, plus the FJX code (that part that was adapted to NO2) and aerosol scattering data for FJX. I hope you get a doi eventually because otherwise it would be impossible to find on the CEDA site.

We will upload the model simulation data to CEDA when preparing the revised manuscript and will ensure that the doi is provided in the revised manuscript. Links will also be provided to the SP2 data (CEDA), aerosol AMS data (available from IAP on request) and aerosol extinction data (available from IAP on request). Links to the ERA5 data set will also be provided here.

Anonymous reviewer 2:

Abstract: The abstract contains a lot of specific results, but some of the key outcomes of the paper get a bit lost in all of the numbers. In addition, the implications receive short shrift. There are many implications regarding potential PM2.5 mitigation strategies that are discussed in Sections 4 and 5 but are not reflected in the abstract.

The main goal of this paper is to highlight the impacts of aerosols on photolysis rates during haze episodes rather than to investigate the potential impacts of $PM_{2.5}$ mitigation strategies. Therefore we have highlighted these key impacts in the abstract. We have edited the last sentence in the abstract highlighting the potential implications that removing aerosol could have on atmospheric oxidants.

'Idealised photochemical box model studies show that such large impacts on photochemistry could lead to a 12% reduction in surface O_3 (3% for OH) due to haze pollution. This therefore highlights that any $PM_{2.5}$ mitigation strategies could have important implications for the oxidation capacity of the atmosphere both at the surface and in the free troposphere.'

Page 2, line 1: Please be specific about what is meant by "very high levels"

In this case we are referring to particulate matter concentrations of greater than 75 μgm^{-3} which corresponds to an AQI of 100. We have clarified this in the revised manuscript.

Page 2, line 29-30: the ")" is missing at the end of "(e.g. strong absorbers such as BC: : :.."

We have corrected this in the revised manuscript

Page 3, lines 25-26: How were the extinction coefficients attributed specifically to anthropogenic aerosols?

The lidar is dual wavelength and measures depolarisation, and attribution of measured backscatter to anthropogenic aerosol was made using the depolarisation ratio. This is described in Yang et al (2010, 2017) who describe the instrument in detail. To clarify this we have altered the final sentence in this paragraph as follows:

'Further details of the lidar instrument, calibration procedures and attribution of extinction coefficients to anthropogenic aerosol using the depolarisation ratio can be found in Yang et al (2010, 2017) and Sugimoto et al. 2002. '

Page 5, lines 23-24: Is "cloud cover" equivalent to "cloud fraction"? If so, the latter term might be clearer since that is (I believe) what is used in Fast-JX.

We have used cloud cover here to refer to the fraction of each layer in the column that is covered by cloud. To clarify this we have revised the manuscript to use cloud fraction.

Page 6, Section 3.1: There is one instance in the entire record where Fast-JX fails to model a significant decrease in photolysis rates when one is observed – May 29th. Are the authors able to comment on what was special about this particular day?

As the model is being driven using ERA5 reanalysis cloud fraction data, this failure to capture the drop in photolysis rates on the 29th May is likely to be due to misrepresentation of the cloud cover in this dataset. Therefore, as Fast-JX is being driven in offline mode, misrepresentation in the

cloud fields will lead to errors in the modelled J rates and thus the model's failure to capture the decrease seen in the observations.

Page 6, line 29: Please add "of each aerosol component" after "vertical profiles and contributions"

We have corrected this in the revised manuscript. Please also see our response to reviewer 1 where we have edited the vertical profiles in the figure to show extinction coefficient rather than AOD. This sentence now reads:

'Figure 2 shows vertical profiles of extinction coefficient for each aerosol component for both campaigns as derived from the optimisation approach described in Section 2.3. Figure 2 also shows the contribution to total column AOD of each aerosol component.'

Page 7, lines 1-2: The wording here makes it seem as though NH4NO3 and organic aerosol make similar contributions as (NH4)2SO4.

The intention here was to indicate that NH_4NO_3 and organic aerosol make similar contributions to each other but not quite as large as those as for $(NH_4)_2SO_4$ and BC. We have rephrased this in the revised manuscript.

Page 7, lines 2-4: I'm not sure I agree with the authors' characterization of the vertical distribution. There is an enhancement of aerosol from 1-2 km that is not as large as in the boundary layer and above 3 km, but does not seem to be consistent with "high values : : : below 1 km which then decline rapidly with altitude before peaking again above 3 km"

In the revised manuscript we have clarified the description of the vertical distribution to indicate that aerosol increases slightly between 1-2 km but this is not as high as values seen in the BL or above 3 km. This sentence reads as follows in the revised manuscript.

"Vertical aerosol extinction profiles show large peaks in both the boundary layer (below 1 km) and above 3 km where there is evidence of an elevated pollution layer (EPL). Elsewhere in the column extinction values are much lower however there are slightly elevated values at 1-2 km, although these are not as large as seen in the boundary layer or EPL."

Page 7, lines 14-16: Can the authors comment on why organic aerosol does not show the same vertical profile as the other aerosols? While the peak values are indeed within the same altitude range as the EPL, there is no layer-like feature in the OA.

The OA does indeed exhibit a different vertical profile to the other species. There are high values in the elevated layer as for other species, but the structure is different, and this suggests that the sources may be rather different (e.g. the influence of biogenic species on the formation of secondary organic aerosol). It could also be linked to factors in the optimisation algorithm which determines the mean scattering efficiency (MSE) of the organic aerosol (Equation 1) and attributes the lidar extinction to each aerosol species.

Page 7, line 31: The word "substantial" has a typo

We have corrected this in the revised manuscript.

Page 7, lines 31-33: Why is the impact on J[NO2] larger than that on J[O1D]?

Generally NO_2 photolysis is more sensitive to scattered radiation than that of O_3 and other species in particular with increasing height above layers of scattering aerosol. This is likely due to the longer wavelength dependence of JNO_2. As JNO_2 occurs largely in the visible part of the spectrum and path length increases with height from the scattering layer, the effects on NO_2 will be amplified compared to those of $J[O^1D]$. This effect is also present at sunrise and sunset.

Page 7, line 33 – Page 8, line 2: The authors state that the surface layer is below the elevated levels of aerosol, but (NH4)2SO4 and BC are still clearly elevated at the surface according to the left panel of Figure 2. Please clarify.

We apologise for the confusion here. The reviewer is correct that aerosol concentrations remain elevated at the surface. This sentence was intended to reflect this and has been corrected in the revised manuscript to read:

"In the surface layer, within the elevated levels of aerosol, the scattering aerosol lead to reductions of -1.7% to -4.4% for $J[O^1D]$ and -3.4% to -7.0% for $J[NO_2]$, with OA producing the largest reduction in both cases."

Page 8, lines 6-7: Here the results in Figure 3 are attributed to "high levels of backscatter from the EPL", but again the OA in Figure 2, 3rd panel does not seem to show a distinct layered structure like the other aerosols do. It seems more accurate to say "from the level of maximum OA" or something similar.

This is correct, the dominant response is from the high maximum level of OA at around 4 km (Figure 2) which is also where the other aerosols exhibit their maximum extinctions in the summer. We have now clarified this sentence to read as follows in the revised manuscript.

"This represents the high levels of backscatter from the level of maximum OA which occurs at a height of approximately 4 km (Figure 2)."

Page 8, lines 19-21: Can the authors elaborate on why the effects of scattering are less pronounced for J[O1D]?

This is due to the longer wavelength dependency of JNO_2 compared to that of $J[O^1D]$. Therefore with increasing path length from the scattering layer the relative impacts on JNO_2 are amplified.

Page 8, lines 31-34: I found the statement that "particulate matter confined mainly to the boundary layer is shown to produce significant impacts at altitude" to be confusing - in much of the preceding discussion, many of the features of Figure 3 were attributed to the EPL during each season, and during summer the EPL seems to dominate the photolysis rate response. I do not see in the analysis provided any example where there is aerosol confined mainly to the boundary layer on which to base this statement.

This statement highlights that the majority of aerosol sources are within the boundary layer. Although most of the impacts of haze pollution (reductions in visibility, health impacts, etc) are at the surface, there is a significant non-local effect of these aerosols at altitude through changes in photolysis rates. We have clarified this sentence in the revised manuscript to reflect this.

Page 9, line 18: It would be helpful to the reader to include a "(not shown)" in the first sentence of the paragraph.

This has been corrected in the revised manuscript.

Page 10, line 20: Please explain briefly what is meant by 'photochemical limitation'.

The term 'photochemical limitation' is used here to indicate that the rate of ozone formation is largely dependent on the amount of incoming radiation. Therefore in the summer months higher incident solar radiation results in higher levels of ozone formation. For clarity, we have amended this sentence in the revised manuscript to read as follows.

"This is important as incoming solar radiation is at its highest during the summer months which results in higher rates of O_3 formation (Tie and Cao, 2009)."

Page 10, lines 24-30: It is clear that China has, in fact, implemented some emissions controls on aerosol precursors (see, for example, Wang et al., ERL, 2015, doi: 10.1088/1748-9326/10/11/114015 and Liu et al., ERL, 2016, doi:10.1088/1748-9326/11/11/114002) and satellite measurements show rapid decreases in NO2 and SO2 from 2011 onward. China's clean air plans (including specific targets for Beijing) should at least be mentioned here. In addition, one of the key points of this study is that the aerosol composition matters, but that aspect is missing here. The differences in aerosol composition between summer and winter appear to make it very unlikely that a single mitigation approach would have substantial impacts in both seasons. Yet the scenarios described here simply assume "reduction of aerosol composition" without regard to species.

The reviewer is correct that China's clean air plans, have seen reduction in aerosol concentrations, in particular the recent drop in $PM_{2.5}$ that has been seen over Beijing. These reductions in particulate concentrations will reduce the attenuation of radiation which in turn will enhance $J[O^1D]$ and JNO_2 at the surface. This will enhance O_3 formation through higher NO levels from JNO_2 photolysis which enhance ozone concentrations through ROO+NO reactions and NO reaction with O_2. Furthermore, enhanced $J[O^1D]$ will lead to higher OH concentrations which can lead to NO_x/HO_x cycling resulting in O_3 formation. We have therefore edited this paragraph to read as follows in the revised manuscript.

'Therefore, under the recent ~30% reduction in $PM_{2.5}$ in Beijing through emissions controls implemented as part of China's clean air plans (Wang et al., 2015; Liu et al., 2016), the resultant increases in $J[O^1D]$ could potentially lead to enhanced O_3 concentrations, where summer levels are already very high (Wang et al., 2006; Xue et al., 2014; Ni et al., 2018). Enhanced near-surface photolysis rates would also increase O_3 production via NO_2 photolysis though this will be partially balanced by the reaction of NO with O_3 itself. However, higher NO levels will also contribute to enhanced O_3 formation through increases in RO_2 and NO reactions. Furthermore, the enhancement of $J[O^1D]$ would increase OH concentrations which would subsequently increase HO_2 and RO_2 and lead to a net rise in O_3 concentrations. In the winter, a similar response would be expected, although due to lower photolysis rates and much lower O_3 concentrations, the effects of particulate control strategies would have a lesser effect on oxidant concentrations.'

With respect the reviewers' comment regarding mitigation strategies targeting individual species, the main aim of this study is to look at the impacts of haze pollution on photolysis rates. The photochemical box model simulation are used as an indication of the potential chemical impacts the presence of aerosols in the urban atmosphere could have. As it is not within scope of the present study we are not evaluating the impacts of different mitigation strategies (and thus strategies targeting individual aerosol species) we do not discuss this here.

Page 11, lines 5-14: Please see the previous comment regarding the lack of a discussion of aerosol composition. Given the focus on composition in this paper, it seems odd to treat aerosol as a singular component.

As the main focus of this study is to focus on the impacts of haze pollution on photolysis rates and not evaluating the impacts of different mitigation strategies we have not focussed on aerosol composition in the simple box model simulations. The main aim of this discussion is to focus on the potential overall effect of aerosols on photochemistry. Due to the complex non-linearities involved in the chemistry a full attribution effect to each aerosol species is beyond the scope of this study. Further to this any aerosol control strategy is likely to reduce all species rather than just one therefore the reduction of all aerosol in the simple box model study is appropriate in this case.

Page 11, lines 25-26: The wording here ("with contrasting results") is very unclear.

We appreciate that this is unclear and have removed the wording "contrasting results" from the sentence in the revised manuscript.

Pages 11-13, Sections 4 and 5: There is some repetition between sections here that could be reduced.

We have tightened up these sections in the revised manuscript to remove the repetition. We have also improved the flow and clarity of the discussion by separating out the box model results into its own sub-section.

Page 13, lines 15-16: I think it would be clearer and more impactful to explicitly say that reducing aerosols (which has a health benefit) would lead to more ozone at the surface (which has a negative health impact) – rather than simply "would offset the photochemical impacts demonstrated here".

Implementing particulate control strategies not only reduces concentrations of aerosols but also the corresponding impacts in photolysis rates. The box model results suggest that this will enhance ozone at the surface but due to the complex non-linearities involved a full quantification of the impacts on ozone concentrations is needed. We have clarified this sentence in the revised manuscript to read.

"Such strategies would not only reduce particulate matter concentrations, but also reduce their impacts on photolysis rates and thus potentially increase surface ozone concentrations."

For clarity we have also separated the conclusions section about the chemical box model results into a new paragraph.

References

Liu, F., Zhang Q., van der A R. J., Zheng, B., Tong D., Yan L., Zheng Y., and He K., Recent reduction in NOx emissions over China: synthesis of satellite observations and emission inventories, Environmental Research Letters, 11, 114002, doi:10.1088/1748-9326/11/11/114002, 2016.

Ni, R., Lin, J., Yan, Y., and Lin,W.: Foreign and domestic contributions to springtime ozone over China, Atmospheric Chemistry and Physics, 18, 11 447–11 469, https://doi.org/10.5194/acp-18-11447-2018, 2018.

Sugimoto, N., Matsui, I., Shimizu, A., Uno, I., Asai, K., Endoh, T., and Nakajima, T.: Observation of dust and anthropogenic aerosol plumes in the Northwest Pacific with a two-wavelength polarization lidar on board the research vessel Mirai, Geophysical Research Letters, 29,7–1–7–4, https://doi.org/10.1029/2002GL015112, 2002.

Tie, X. and Cao, J.: Aerosol pollution in China: Present and future impact on environment, Particuology, 5 7, 426 – 431, https://doi.org/https://doi.org/10.1016/j.partic.2009.09.003, 2009.

Wang, T., Ding, A., Gao, J., and Wu, W. S.: Strong ozone production in urban plumes from Beijing, China, Geophysical Research Letters, 33, https://doi.org/10.1029/2006GL027689, 2006.

Wang, S., Zhang, Q., Martin, R.V., Philip, S., Liu, F., Li M., Jiang X., He, K., Satellite measurements oversee China's sulfur dioxide emission reductions from coal-fired power plants, Environmental Research Letters, 10, 114015, doi:10.1088/1748-9326/10/11/114015, 2015.

Xue, L. K., Wang, T., Gao, J., Ding, A. J., Zhou, X. H., Blake, D. R., Wang, X. F., Saunders, S. M., Fan, S. J., Zuo, H. C., Zhang, Q. Z., and Wang, W. X.: Ground-level ozone in four Chinese cities: precursors, regional transport and heterogeneous processes, Atmospheric Chemistry and Physics, 14, 13 175–13 188, https://doi.org/10.5194/acp-14-13175-2014, 2014.

Yang, T., Wang, Z., Zhang, B., Wang, X., Wang, W., Gbauidi, A., and Gong, Y.: Evaluation of the effect of air pollution control during the Beijing 2008 Olympic Games using Lidar data, Chinese Science Bulletin, 55, 1311–1316, https://doi.org/10.1007/s11434-010-0081-y, 2010.

Yang, T., Wang, Z., Zhang, W., Gbaguidi, A., Sugimoto, N., Wang, X., Matsui, I., and Sun, Y.: Technical note: Boundary layer height determination from lidar for improving air pollution episode modeling: development of new algorithm and evaluation, Atmospheric Chemistry and Physics, 17, 6215–6225, https://doi.org/10.5194/acp-17-6215-2017, 2017.

Photochemical impacts of haze pollution in an urban environment

Michael Hollaway[1,a], Oliver Wild[1], Ting Yang[2], Yele Sun[2,3], Weiqi Xu[2,3], Conghui Xie[2,3], Lisa Whalley[4,5], Eloise Slater[4], Dwayne Heard[4,5], and Dantong Liu[6,7]

[1]Lancaster Environment Centre, Lancaster University, Bailrigg, Lancaster, UK
[2]State Key Laboratory of Atmospheric Boundary Layer Physics and Atmospheric Chemistry, Institute of Atmospheric Physics, Chinese Academy of Sciences, Beijing 100029, China
[3]University of Chinese Academy of Sciences, Beijing 100049, China
[4]School of Chemistry, University of Leeds, Leeds, UK
[5]National Centre for Atmospheric Science, University of Leeds, Leeds UK
[6]Department of Atmospheric Sciences, School of Earth Sciences, Zhejiang University, Hangzhou, Zhejiang, China
[7]Centre for Atmospheric Sciences, School of Earth and Environmental Sciences, University of Manchester, Manchester, UK
[a]Now at: Centre for Ecology & Hydrology, Lancaster Environment Centre, Bailrigg, Lancaster, UK.

Correspondence: Michael Hollaway (m.hollaway@lancaster.ac.uk)

Abstract. Rapid economic growth in China over the past 30 years has resulted in significant increases in the concentrations of small particulates ($PM_{2.5}$) over the city of Beijing. In addition to health problems, high aerosol loading can impact visibility and thus reduce photolysis rates over the city leading to potential implications for photochemistry. Photolysis rates are highly sensitive not only to the vertical distribution of aerosols but also to their composition as this can impact how the incoming solar radiation is scattered or absorbed. This study, for the first time, uses aerosol composition measurements and lidar optical depth to drive the Fast-JX photolysis scheme and quantify the photochemical impacts of different aerosol species during the Air Pollution and Human Health (APHH) measurement campaigns in Beijing in November–December 2016 and May–June 2017. This work demonstrates that severe haze pollution events ($PM_{2.5}$ > 75 μgm^{-3}) occur during both winter and summer leading to reductions in O_3 photolysis rates of ~~27.4–34.0~~27–34 % (greatest in winter) and reductions in NO_2 photolysis of ~~40.4–66.2~~40–66 % (greatest in summer) at the surface. It also shows that in spite of much lower $PM_{2.5}$ concentrations in the summer months, the absolute changes in photolysis rates are larger for both O_3 and NO_2. In the winter absorbing species such as black carbon dominate the photolysis response to aerosols leading to mean reductions in $J[O^1D]$ and $J[NO_2]$ in the lowest 1 km of ~~23.8~~24 % and ~~23.1~~23 % respectively. In contrast in the summer, scattering aerosol such as organic matter dominate the response leading to mean decreases of ~~2.0–3.0~~2–3 % at the surface and increases of ~~8.4–10.1~~8–10 % at higher altitudes (3–4 km). During these haze events in both campaigns, the influence of aerosol on photolysis rates dominates over that from clouds. These large impacts on photochemistry can have ~~important~~ significant implications for concentrations of important atmospheric oxidants such as the hydroxyl radical. Idealised photochemical box model studies show that such large impacts on photochemistry could lead to a 12 % reduction in surface O_3 (3 % for OH) due to haze pollution. This therefore highlights that any $PM_{2.5}$ mitigation strategies could have important implications for the oxidation capacity of the atmosphere both at the surface and in the free troposphere.

1 Introduction

As a result of rapid economic growth and industrialisation over the past 30 years, air pollution has become a major problem in China (Chan and Yao, 2008; Zhang et al., 2015), with an increase in the number of haze episodes emerging as a particular issue. During such haze events, concentrations of small aerosol particles ($PM_{2.5}$: particles with an aerodynamic diameter of less than 2.5 μm) can climb to very high levels ~~(Han et al., 2015; Wang et al., 2018)~~ (higher than 75 μgm^3; Han et al. (2015); Wang et al. (2018)) leading to significant reductions in visibility, health problems and potential feedbacks on atmospheric chemistry and dynamics (Cheng et al., 2011; Han et al., 2015; Lelieveld et al., 2015; Xing et al., 2017).

High aerosol loadings not only impact dynamics through their regulation of the atmospheric radiation budget ~~(Kaiser and Qian, 2002; Hu~~ (Kaiser and Qian, 2002; Martin et al., 2003; Bian et al., 2003; Hu et al., 2017), but can also have significant impacts on atmospheric oxidation capacity through reductions in photolysis rates (Liao et al., 1999; Lou et al., 2014; Tang et al., 2003; Li et al., 2011; Xing et al., 2017). Photolysis plays a very important role in initiating atmospheric photochemistry. Of particular importance are the photolysis of NO_2 in the troposphere ($J[NO_2]$), which is key to chemical generation of ozone (O_3) and the photolysis of O_3 itself ($J[O^1D]$) to produce electronically excited oxygen (O^1D). O^1D may subsequently react with water vapour and is the main source of the hydroxyl radical (OH) in the atmosphere globally. In addition, in highly polluted urban environments such as Beijing, photolysis of nitrous acid (HONO) is also a major source of OH. OH is highly reactive and serves as the primary oxidation sink of many atmospheric species whilst also playing a key role in initiating catalytic cycles that result in poor air quality (e.g. O_3 formation).

Both the vertical distribution and composition of aerosols can impact how incoming solar radiation is absorbed or scattered throughout the atmospheric column which in turn can significantly affect photolysis rates (Tang et al., 2003; Li et al., 2011). For example, Li et al. (2011) estimated that $J[O^1D]$ rates over Eastern China were reduced by 53 %, 37 % and 21 % in the lower, middle and upper troposphere during high summer aerosol loadings in 2006. This resulted in corresponding OH concentration reductions of 51 %, 40 % and 24 % respectively. Therefore, vertical characterisation of aerosols is critical to fully understanding the impact of severe haze on atmospheric photochemical processes. The key processes behind the formation and composition of severe haze events over China at ground sites (including in Beijing) have been studied extensively (Han et al., 2015; Huang et al., 2014; Ji et al., 2014; Zhao et al., 2013; Sun et al., 2013), with some studies also using aircraft and tethered balloon measurements to investigate the vertical profiles of aerosol and gaseous pollutants (Chen et al., 2009; Zhang et al., 2009; Ran et al., 2016; Li et al., 2015). Aircraft typically only permit measurements above 300 m altitude and fail to capture the full evolution of aerosol profiles and tethered balloons are normally operated in rural settings that are not representative of urban environments. Therefore, greater understanding of the vertical distribution of aerosol loadings is still required.

Recent studies have better captured the evolution of black carbon (BC) profiles and their associated optical impacts during haze events over Beijing (Wang et al., 2018), but these are still limited to the lower boundary layer (< 260 m altitude). Lidar instruments are useful in providing vertical profiles of total aerosol extinction and have been applied over Beijing previously (Yang et al., 2010, 2017) to measure up to a height of 6 km. However, only the total extinction can be retrieved and there is no information on the contribution from different aerosol species (e.g. strong absorbers such as BC or scattering aerosol such as

ammonium sulphate, $(NH_4)_2SO_4$), which is required to understand how the incoming solar radiation is scattered and absorbed. As a result, atmospheric models are often used to simulate aerosol distributions and composition throughout the atmospheric column and their impacts on photolysis rates (Tang et al., 2003; Li et al., 2011). However, such model studies often are often poorly constrained by observations (particularly in the upper atmosphere) and can fail to accurately predict peaks in aerosol concentrations during severe haze events (Wang et al., 2014b, a, c; Zheng et al., 2015).

In this study, aerosol composition and lidar extinction measurements from two intensive field campaigns conducted in Beijing in Winter 2016 and Summer 2017 are used to derive chemically apportioned vertical profiles of aerosol extinction. These profiles are used, for the first time, to critically test an offline photolysis scheme against measurements of photolysis rates under observed aerosol loadings and to quantify the contribution of different aerosol components to changes in photolysis rates. This enables a better understanding of the impacts of severe haze episodes on pollutant photochemistry in contrasting seasons and provides insight into the photochemical implications of potential future pollution reduction strategies.

2 Materials and Methods

2.1 Measurement campaigns and sampling site

Two measurement campaigns were conducted at the tower site of the Institute of Atmospheric Physics, Chinese Academy of Sciences (IAP-CAS) as part of the joint UK-China Air Pollution and Human Health (APHH) programme addressing the sources, processing and impacts of air pollution in Beijing (Shi et al., 2019). The site is located in urban surroundings (39.6° N, 116.2° E) between the third and fourth ring roads in the ~~North~~ north of Beijing, 40 m from the nearest road and around 400 m from the Jingzang Highway (Han et al., 2015). The first campaign was conducted from 5th November to 10th December 2016 and the second campaign was conducted from 15th May to 22nd June 2017 in order to monitor haze episodes during different seasons (Shi et al., 2019).

2.2 Instrumentation

Non-refractory aerosol species (including sulfate, nitrate, chloride, ammonium and organics) and black carbon (BC) were measured using an Aerodyne High-Resolution Time-of-Flight Aerosol Mass Spectrometer (HR-ToF-AMS; DeCarlo et al., 2006) and a 7-wavelength Aethalometer (model AE33; Magee Scientific Corp., Drinovec et al., 2015) respectively, which provided aerosol composition data at 5 minute resolution. Total aerosol extinction and aerosol absorption were measured simultaneously at 870 nm using a Photoacoustic Extinctiometer (PAX; Droplet Measurement Technologies, Boulder, CO, USA), with data reported for dry aerosol (approximately 40% relative humidity) at 5 minute resolution. The PAX, HR-ToF-AMS and Aethalometer were all located on the roof of a three floor laboratory building at the tower site.

Vertical profiles of aerosol extinction were obtained using a dual-wavelength (1064, 532 nm) depolarisation lidar which was located at a height of 28 m on the roof of a building near the aerosol monitoring equipment. The lidar provided extinction coefficients attributed to anthropogenic aerosols at 30 m vertical resolution up to an altitude of 6 km and 15 minute temporal

resolution for both campaign periods. Further details of the lidar instrument~~and calibration procedures~~, calibration procedures and attribution of extinction coefficients to anthropogenic aerosol using the depolarisation ratio can be found in Yang et al. (2010, 2017) and Sugimoto et al. (2002).

The spectrally resolved ($\approx$ 1 nm) actinic flux was measured during both campaign periods at a temporal frequency of 1 minute using a spectrometer (Ocean Optics QE65000) which was fibre-coupled to a 2pi quartz receiver optic (Meteorologie Consult GmbH). J[O^1D] and J[NO_2] rates were then calculated using literature values of wavelength dependent photodissociation quantum yields and absorption cross-sections (Whalley et al., 2018). The instrument provided measurements representative of a height of 3.5 m above ground level.

Finally, a single particle soot photometer (SP2) instrument was used to measure the physical properties of individual black carbon (BC) particles during each campaign period. Described in detail by Liu et al. (2010, 2014), the SP2 employs a laser at 1064 nm to detect the optical properties of BC particles including core diameter and coating thickness for each single particle. The core size and coating information for BC covering both the winter and summer campaign periods is presented in detail in Liu et al. (2018a).

2.3 Chemical apportionment of aerosol extinction

To estimate the vertical extinction profile for each species, it is necessary to chemically apportion the total aerosol extinction measured with the lidar in the 532 nm channel. The co-located PAX, HR-ToF-AMS and Aethelometer data are used here to develop an empirical relationship between aerosol composition and optical properties.

Based on the assumption that aerosol particles are externally mixed and that the extinction of individual species are independent of one another, the contribution of the non-refractory aerosol species to the total extinction coefficient (b_{ext}) is estimated at 870 nm. A differential evolution optimisation algorithm is utilised on the scattering coefficient (b_{sct}) and the respective concentrations of ammonium sulfate ($(NH_4)_2SO_4$), ammonium nitrate (NH_4NO_3), ammonium chloride (NH_4Cl) and organic aerosol (OA). The concentration of the inorganic aerosol components ~~was~~ are calculated from the measurements of sulfate, nitrate and chloride assuming that these ions are neutralised by ammonium.

The scattering coefficient b_{sct} is assumed to be the difference between b_{ext} and the absorption coefficient (b_{abs}) measured by the PAX instrument. As the algorithm is applied to lidar measurements in ambient conditions, the effects of aerosol hygroscopic growth needs to be accounted for through use of the humidity dependent growth factor (f_{RH}). This work uses the f_{RH} factor from the Interagency Monitoring of Protected Visual Environments (IMPROVE) algorithm (Pitchford et al., 2007) which has previously been used to chemically apportion PM extinction over China (Shen et al., 2014). As in the IMPROVE algorithm, the effects of hygroscopic growth are only allowed to impact the inorganic ions. The differential algorithm is calibrated using an optimisation approach to minimize the mean absolute error between the observed scatter (b_{sct}) and the value estimated with the differential evolution algorithm. This allows the mass scattering efficiency (MSE) for each species to be estimated.

For the contribution of BC to overall extinction, it is assumed that all absorption from the PAX measurements can be attributed to BC, following the approach of Han et al. (2015). A simple linear regression model is fitted between the absorption coefficient (b_{abs}) and the measured BC mass concentration. The slope of this regression yields the mass absorption efficiency

(MAE) for BC. Combining the calculated MSE and MAE values for each PM constituent gives the following empirical relationships for the winter (Eqn 1) and summer (Eqn 2) campaigns. Here the values in square brackets represent the concentrations of each PM constituent (μgm^{-3}), the numbers represent the optimised MSE/MAE values (m^2g^{-1}) and f_{RH} represents the hygroscopic growth factor.

$$b_{sct_{win}} = 4.0 * f_{RH} * [(NH_4)_2SO_4] + 1.1 * f_{RH} * [(NH_4)NO_3] + 0.3 * f_{RH} * [(NH_4)Cl] + 1.0 * [OA] + 3.3 * [BC] \quad (1)$$

$$b_{sct_{sum}} = 4.6 * f_{RH} * [(NH_4)_2SO_4] + 5.5 * f_{RH} * [(NH_4)NO_3] + 5.0 * f_{RH} * [(NH_4)Cl] + 1.8 * [OA] + 8.8 * [BC] \quad (2)$$

An optimisation approach is then used to estimate the contribution of each species to the measured lidar extinction at each 30 m layer (up to a height of 6 km) given the empirical relationships derived in Equations 1 and 2. In this case the assumption is made that the MSE and MAE values for each species hold with height. Relative humidity is obtained for the column from the European Centre for Medium-range Weather Forecast (ECMWF) ERA5 dataset (ECMWF, 2018) and is mapped onto the lidar height levels in order to estimate the change in the f_{RH} with height and thus the effects of hygroscopic growth on the inorganic aerosol species. As the lidar operates at 532 nm and the PAX optical properties are measured at 870 nm, the lidar extinction is scaled to the PAX wavelength using the Angstrom exponent from a nearby Aerosol Robotic Network (AERONET) station (Beijing CAMS) before the optimisation. Overall, this provides vertical profiles of extinction attributed to each aerosol species which are then converted to aerosol optical depth (AOD) by integrating over each 30 m layer.

2.4 Model Description and setup

Fast-JX is an interactive photolysis scheme designed to efficiently and accurately calculate photolysis rates for use in global atmospheric models at minimal computational cost (Wild et al., 2000; Bian and Prather, 2002; Neu et al., 2007; Prather, 2015). The scheme apportions light from wavelengths 177 to 850 nm into 18 bins to permit calculation of photolysis rates appropriate to both tropospheric and stratospheric chemistry. Cloud and aerosol optical depths are used along with the scattering phase functions for appropriate particle types to solve the 8-stream multiple scattering problem (Wild et al., 2000). This allows calculation of the photolytic intensity which can be used to determine photolysis rate coefficients for key atmospheric species (e.g. J[O^1D] and J[NO_2]). The scheme also utilises a quadrature approach to ~~account for~~ average over multiple layers of overlapping clouds ~~(Prather, 2015)~~(Neu et al., 2007; Prather, 2015).

The Fast-JX scheme is run here in 'stand-alone' mode using offline data rather than run interactively within a chemical transport model (CTM) framework. This allows it to be constrained using observations where these are available. In this study, the optical depths for aerosols from the lidar chemical apportionment are used in conjunction with data on cloud (cloud ~~cover~~fraction, liquid water content and ice water content) and meteorological variables (temperature and relative humidity)

from the ERA5 reanalysis dataset (ECMWF, 2018). Cloud cover from each ERA5 layer is used to drive Fast-JX using the above mentioned quadrature approach for overlapping layers. Atmospheric columns of O_3 and NO_2 are provided from the ERA5 and the CAMS reanalysis datasets (CAMS, 2018; Inness et al., 2018) respectively, to account for absorption from gas-phase species. Due to high concentrations of NO_2 in Beijing, particularly in the boundary layer, the standard version of the Fast-JX code was modified to account for the significant attenuation that can occur when photons are absorbed by NO_2. In addition, the scattering phase function for BC was updated to account for the ageing and coating of BC particles. This is done using the BC core size and coating thickness determined from SP2 measurements to derive asymmetry parameters at each Fast-JX wavelength. These asymmetry parameters were used to estimate the first eight terms of the scattering phase function using a Legendre expansion of the Henyey-Greenstein function (Henyey and Greenstein, 1941).

3 Results

In order to critically evaluate the impact of haze pollution events on photolysis rates during the winter and summer campaign periods, a range of different scenarios are run (Table 1). These include runs where the radiative effects of each key aerosol species and clouds are switched on in isolation. This enables the contributions of clouds and aerosols to be determined, and for the contribution of key aerosol species to be identified respectively. The scenario where both cloud and aerosol effects are turned on represents the best model simulation of photolysis rate constants during the campaigns and allows critical evaluation of the model against observed values of $J[O^1D]$ and $J[NO_2]$.

3.1 Fast-JX evaluation

Observed $J[O^1D]$ and $J[NO_2]$ are captured well by the model during both the winter and summer periods, as shown in Figure 1. In general, when the sun is highest in the sky at local noon, Fast-JX tends to capture observed $J[O^1D]$ within 8 % (+3.7 % bias in summer and +7.8 % bias in winter, averaged over all days), marginally higher than observations in both cases. For $J[NO_2]$ the model performance is much better during the summer campaign (~~positive bias of~~ +5.6 % bias) than the winter (~~bias of~~ +20.4 % bias). In the summer, on clear sky days (28th May, 1st, 7th, 9th, 14th, 15th and 16th June) the model performs slightly less well for $J[O^1D]$ (+5.5 % average bias) and slightly better for $J[NO_2]$ (+4.7 % bias). In contrast, on winter clear sky days (19th, 22nd, 27th November and 1st December) the model performs better for $J[O^1D]$ (+2.7 % bias) but less well for $J[NO_2]$ (+23.1 % bias). These discrepancies may be linked to uncertainties in the retrieval of AOD from the lidar instrument and therefore to underestimation of the background aerosol on these less polluted days. In addition, errors in the column O_3 from the ERA5 reanalysis could be responsible for the positive bias of model $J[O^1D]$. However, the ERA5 column O_3 was independently validated against Brewer measurements over Beijing which indicated that the total column was captured well by the reanalysis product (mean bias of -2.0 % for summer and +3.4 % for winter), indicating that this is likely to be a smaller source of error. There are also issues with stray light during calibration of the spectrometer instrument at shorter wavelengths (below 300 nm) which may affect the fluxes derived in this part of the spectrum and thus the measured photolysis rates, particularly for $J[O^1D]$. Overall, however, the model is shown to perform reasonably well, capturing the magnitude of the reductions in photolysis rates

observed during severe haze episodes in both winter (16^{th}–18^{th}, 20^{th} and 29^{th} November) and summer periods (6^{th}, 22^{nd} and 23^{rd} June). This is particularly important during the summer where photochemistry is most active and large reductions in photolysis rates can have important impacts on oxidant concentrations and the production and destruction of key pollutants (e.g. O_3 and secondary organic aerosol formation).

3.2 Chemical apportionment of AOD

Figure 2 shows ~~the vertical profiles and contributions to total column AOD for~~ vertical profiles of extinction due to aerosol for each $PM_{2.5}$ component for both campaigns as derived from the optimisation approach ~~described~~ described in Section 2.3. Figure 2 also shows the contribution to total column AOD of each aerosol component. The differences between haze periods and non-haze periods are also highlighted. Haze is defined here as conditions where the $PM_{2.5}$ concentration is larger than 75 μgm^{-3} (corresponding to an air quality index, AQI, of 100) which is the daily air quality limit for China (Shi et al., 2019). In winter $(NH_4)_2SO_4$ (~~39.1~~39 %) and BC (~~30.5~~31 %) provide the largest contributions to total column AOD during haze periods with NH_4NO_3 and organic aerosol making ~~similar contributions (13.1~~the second largest contributions (13 % and ~~12.3~~12 % respectively) and NH_4Cl making the smallest ~~contribution (5.0~~(5 %). Vertical ~~AOD profiles show high values in~~ aerosol extinction profiles show large peaks in both the boundary layer (below 1 km~~which then decline rapidly with altitude before peaking again~~) and above 3 km where there is evidence of an elevated pollution layer (EPL). Elsewhere in the column extinction values are much lower however there are slightly elevated values at 1-2 km, although these are not as large as seen in the boundary layer or EPL. This phenomenon has been demonstrated previously in stable conditions during haze episodes when the topography around Beijing can lead to the Mountain Chimney effect where pollutants build up in elevated layers rather than disperse through the free troposphere (Chen et al., 2009; Liu et al., 2018b). During cleaner winter periods $(NH_4)_2SO_4$ (~~29.8~~30 %) and BC (~~23.2~~23 %) still dominate total column AOD and NH_4NO_3 and organic aerosol make very similar contributions to those during haze periods (~~12.9~~13 % and ~~14.3~~14 %). However, in contrast to haze periods, NH_4Cl makes the third biggest contribution at ~~19.8~~20 %. As these cleaner periods are ~~charaterised~~ characterised by lower levels of particulates and more unstable conditions, AOD values are in general much lower than in hazy conditions and the largest values are seen within the boundary layer.

During the summer campaign, in both haze and cleaner periods, organic matter dominates the contribution to total column AOD (~~37.9~~38 % and ~~44.2~~44 % respectively) with $(NH_4)_2SO_4$ providing the second largest contribution (~~21.0~~21 % and ~~15.5~~16 % respectively). BC is shown to contribute less to AOD during haze days (~~6.6~~7 %) than in cleaner periods (~~12.7~~13 %). In contrast to the winter, the highest AOD values in hazy periods are seen in an EPL which lies between 3–5 km and is dominated by BC and organic matter, although all other species are also elevated. Although haze conditions occur much less frequently in the summer campaign, the ~~AOD~~ extinction values for BC and organic matter at these higher levels are comparable to those seen in the winter months, with peaks of around ~~0.015~~60 Mm^{-1}. During the summer campaign, all species except organic matter show much lower AOD values during the cleaner periods than during haze, and there is little indication of an EPL layer. There is substantial organic matter still present in these cleaner periods, and this is maximum at 2–3 km where AOD values peak at around ~~0.006~~ 20 Mm^{-1} (higher than during cleaner periods in the winter campaign). Finally, to check consistency, the

total column optical depth from the lidar was compared to AERONET values at a nearby site (Beijing CAMS) showing good agreement for both campaigns.

3.3 Impacts of aerosol species on photolysis rates in haze conditions

As Fast-JX is run in offline mode, the effects of each aerosol species can be determined independently~~, and the impacts under haze conditions are shown in~~. Each aerosol species is allowed to influence incoming solar radiation in isolation (Table 1) allowing the change in photolysis rates with respect to clear sky conditions to be quantified (Figure 3). This allows quantification of the impacts of each species on photolysis rates during haze episodes in Beijing. During winter, absorption by BC has the greatest impact on both $J[O^1D]$ and $J[NO_2]$, resulting in ~~23.8~~24 % and ~~23.1~~23 % reductions in the lowest 1 km respectively, compared to clear sky conditions. The impact of BC reduces with height, but continues to show the largest response up to 4 km for $J[O^1D]$ (~~-5.7~~-6 %) and 3 km for $J[NO_2]$ (~~-6.3~~-6 %). At higher altitudes the effects of scattering aerosol begin to dominate, with a general enhancement in photolysis rates compared to clear sky conditions of ~~1.3–3.8~~1–4 % for $J[O^1D]$ and ~~1.5–6.8~~2–7 % for $J[NO_2]$. The most pronounced effects are seen towards the top of the lidar column (6 km), where there is ~~substnatial~~ substantial backscattered solar radiation from the polluted boundary layer below. The largest increases are due to $(NH_4)_2SO_4$ (~~3.8~~4 % for $J[O^1D]$ and ~~6.8~~7 % for $J[NO_2]$) which corresponds to the presence of large amount of $(NH_4)_2SO_4$ in the EPL during haze periods in winter (Figure 2). In the surface layer, ~~below~~ within the elevated levels of aerosol, the scattering aerosol lead to reductions of ~~-1.7~~-2 % to ~~-4.4~~-4 % for $J[O^1D]$ and ~~-3.4~~-3 % to ~~-7.0~~-7 % for $J[NO_2]$, with OA producing the largest reduction in both cases.

In contrast, during the summer, scattering by OA dominates the response of both $J[O^1D]$ and $J[NO_2]$. At the surface, OA leads to a ~~2.9~~3 % reduction in $J[O^1D]$ and a ~~2.4~~2 % reduction in $J[NO_2]$. Higher up the column, within and above the EPL layer, scattering aerosol leads to increases in photolysis for both species, with the effects of OA producing the dominant response (~~3.7–8.4~~4–8 % for $J[O^1D]$ and ~~4.3–10.1~~4–10 % for $J[NO_2]$). This represents the high levels of backscatter from the ~~EPL layer during haze events in the summer campaign~~level of maximum OA which occurs at a height of approximately 4 km (Figure 2). Overall, the relative impacts of the scattering aerosol compared with clear sky conditions are similar in winter and summer, but due to the higher rates of photolysis in summer the absolute impacts are much larger. Absorption by BC is still evident during the summer leading to reductions in photolysis of ~~0.1–2.4~~0–2 % for $J[O^1D]$ and ~~1.0–3.8~~1–4 % for $J[NO_2]$. However, in contrast to winter, the impacts of BC are lower than those of OA in all layers with exception of $J[NO_2]$ in the surface layer.

3.4 Diurnal impacts of aerosols on photolysis rates

Figure 4 shows the impacts of all aerosol on the vertical profiles of $J[O^1D]$ and $J[NO_2]$ for each daylight hour averaged over each campaign period. During the winter, the strong effect of absorption by BC is evident for both $J[O^1D]$ and $J[NO_2]$ with reductions in excess of ~~20.0~~20 % in the lowest 500 m and reaching maximum reductions of ~~34.0~~34 % (1.7×10^{-6} s^{-1}) for $J[O^1D]$ and ~~40.4~~40 % (1.6×10^{-3} s^{-1}) for $J[NO_2]$. Reductions in $J[NO_2]$ show a stronger diurnal pattern over the day, with the greatest effects around sunrise, where reductions of ~~as much as 20.0~~at least 5.0×10^{-4} ~~%~~ s^{-1} are seen up to an altitude of 5 km. This is when the atmospheric path is at its longest and absorbing species such as BC have a more dominant effect. Approaching

noon, the effects of scattering aerosol start to dominate down through the column and this results in increases in $J[NO_2]$ to a maximum of 10.5 % ($1.1x10^{-3}$ s^{-1}) at 6 km altitude. For $J[O^1D]$ the effects of scattering are less pronounced and absorption continues to dominate below 3 km. The effects of scattering are more evident above this level, and $J[O^1D]$ is enhanced by around 6.0 % ($1.0x10^{-6}$ s^{-1}) during the middle of the day.

During the summer, the responses of $J[O^1D]$ and $J[NO_2]$ are similar, with the absorption effect of BC evident in a very shallow surface layer about 200–300 m deep. The exception to this is around sunrise and sunset where reductions in photolysis rates extend to altitudes of 2–3 km. In this layer, reductions in photolysis rates for both species are in excess of 20.0 %, and these are most pronounced for $J[NO_2]$ where reductions reach 66.0 % ($1.6x10^{-3}$ s^{-1}). The effects of scattering aerosol are more pronounced during the summer than the winter and are seen much lower in the column, particularly during the middle of the day. The impacts on $J[NO_2]$ are slightly greater than for $J[O^1D]$, with increases of 10.0–15.0 % ($1.0x10^{-3}$ to $2.0x10^{-3}$ s^{-1}) compared with 5.0–10.0 % ($1.5x10^{-6}$ to $3.0x10^{-6}$ s^{-1}) at 1–6 km altitude. Although these increases are not as large as the reductions seen in the boundary layer, they have the potential to have significant impacts on chemical processes through influences on oxidant concentrations. This can have further impacts on lifetimes of other pollutants in the free troposphere. These findings also allow quantification of the full impacts of haze pollution throughout the lower troposphere and highlight the non-local impacts of aerosols. ~~That is that particulate matter confined mainly to the boundary layer is shown to produce~~ This shows that aerosols, whose origin are mainly from the surface (within the boundary layer), not only impact visibility and photolysis at the surface but can also have significant impacts at altitude. This extends findings of previous studies that largely focus on the impacts of haze pollution on surface photolysis rates and not those throughout the free troposphere (Li et al., 2005; Xing et al., 2017).

3.5 Cloud vs aerosol impacts during campaign periods

The average impacts of clouds and aerosol on $J[O^1D]$ and $J[NO_2]$ are shown for both campaigns for haze days in Figure 5. During the winter, aerosols produce reductions of more than ~~30.0~~30 % at the surface for both photolysis rates. The impact of clouds in this lowest layer is much smaller, with reductions of around 7 % for both species. At higher altitudes, the effects of aerosol are less dominant and backscatter from clouds is more evident, leading to increases in photolysis rates for both species. The largest increases are seen in the 1–2 km layer where photolysis rates increase by ~~46.4–57.5~~46–58 % with the impacts for $J[NO_2]$ slightly larger than for $J[O^1D]$. The effects of cloud backscatter are smaller higher up the column, and increases of ~~17.0–31.9~~17–32 % are seen in the 5–6 km layer, with largest impacts again seen for $J[NO_2]$. This pattern is reflected in the combined impact of cloud and aerosol which shows ~~33.3–34.4~~33–34 % reductions in the surface layer, ~~32.0–41.7~~32–42 % increases in the 1–2 km layer, and smaller ~~19.9–39.3~~20–39 % increases in the 5–6 km layer.

In summer, during haze conditions, clouds produce the largest ~~impact~~ impacts on photolysis rates in the surface layer ~~, with approximately twice the impact of aerosols~~ (reductions of ~~11.3–10.2~~10–11 %~~compared to ≈6.1~~), approximately double that attributed to aerosol (6 %). The effects of high levels of scattering aerosol (particularly OA) during ~~summer haze~~ these conditions are evident higher in the column where ~~the~~ increases in photolysis rates due to aerosol are much larger than ~~that~~ those from clouds. ~~This is reflected in the~~ The combined effects of cloud and ~~aerosols which see reductions in photolysis rates in~~ aerosol are reductions in the lowest 3 ~~km (0.1–17.2~~km (0–17 % for $J[O^1D]$ and ~~1.2–15.7~~1–16 % $J[NO_2]$) ~~switching to increases~~

from 3–6 km (8.8–13.7which are dominated by the influence of clouds. Between 3-6 km the effects of backscatter from aerosol are greater than those from clouds giving net increases in photolysis rates (9–14 % for $J[O^1D]$ and 11.3–17.811–18 % $J[NO_2]$)where the backscatter from aerosol dominates over that from clouds.

When the impacts are averaged over all days in each campaign period (not shown), an interesting picture emerges. In the winter, aerosol produce the largest impacts in the surface layer (-15.9-16 % for $J[O^1D]$ and -17.3-17 % $J[NO_2]$), with the effects of cloud more dominant at higher altitudes (14.8–26.215–26 % for $J[O^1D]$ and 25.6–34.726–35 % $J[NO_2]$). This shows that background levels of aerosol during the winter, even at levels below that classified as haze, are sufficiently high to produce a greater impact on photolysis than clouds. As shown in Figure 2, a polluted layer consisting mainly of BC and $(NH_4)_2SO_4$ is present in the lowest 1 km even on non-haze days, and this most likely contributes to the dominant effect of aerosol at the surface. For the summer campaign, averaged over all days, cloud impacts dominate over aerosol impacts throughout the column for both species, consistent with the findings of Hall et al. (2018). However, the presence of an elevated layer of OA (Figure 2) at 2–3 km is evident on the non-haze days where aerosol and clouds produce comparable increases in photolysis rates (-5.05 % for $J[O^1D]$ and -7.07 % for $J[NO_2]$).

4 Discussion

This study presents an in-depth investigation into the impacts of haze pollution on photolysis rates during two intensive field campaigns (Winter 2016 and Summer 2017) in Beijing. For the first time, an observation driven approach is used to quantify how different aerosol species contribute to changes in photolysis rates and to explore how they influence photochemistry during haze events in a megacity.

On haze days, in the winter and summer campaign periods, aerosols show distinct and contrasting impacts on $J[O^1D]$ and $J[NO_2]$. The effects of absorbing species such as BC dominate during the winter leading to large reductions in $J[O^1D]$ and $J[NO_2]$ in the lowest 1 km of 23.824 % and 23.123 % respectively. During the summer scattering aerosol dominates with OA producing the largest response throughout the column leading to reductions of 2.9–2.4around 3 % in the lowest 1 km and increases of -10.0around 10 % at 3–4 km. These differences largely reflect the different pollution sources during the campaign periods with high levels of coal burning during the winter season leading to large emissions of soot (BC) and high production of $(NH_4)_2SO_4$ particles. During the summer, emissions of biogenic volatile organic compounds (bVOCs) are much larger leading to formation of secondary organic aerosol (Mentel et al., 2013; Riipinen et al., 2011) which can account for the dominance of OA in this season.

To test the sensitivity of the results to assumptions about the mixing state of aerosol, an additional simulation was performed treating BC as externally mixed rather than internally mixed, following Liao et al. (1999). With externally mixed BC, the effects of the absorbing species still dominate the response of photolysis rates during the winter campaign, see Figure 3. However, the magnitudes of reductions in the lowest 1 km for both $J[O^1D]$ and $J[NO_2]$ is larger (44.044 % and 45.045 % respectively) than when the BC is assumed to be coated (23.824 % and 23.123 % respectively). In the summer, the effect of externally mixed BC

leads to a slightly larger contribution from BC to reductions in J[O^1D] and J[NO_2] throughout the column, although OA still provides the dominant response for both species (Figure 3).

It is also demonstrated that despite particulate levels being lower on average during the summer months, haze events where the AQI is higher than 100, still occur. On haze days the mean relative impacts of aerosols on photolysis rates is lower in summer than in winter, with reductions in J[O^1D] of just ~~6.1~~6 % in the surface layer compared to ~~28.5~~29 % in winter. However, summer J[O^1D] values in this layer are an order of magnitude higher than in winter ($1.6x10^{-5}s^{-1}$ compared to $2.6x10^{-6}s^{-1}$) and so the absolute changes are higher in summer ($1.0x10^{-6}s^{-1}$ compared to $7.4x10^{-7}s^{-1}$). This is important as incoming solar radiation is at its highest during the summer months ~~and is often the 'photochemical limitation' in the formation of O_3 (Tie and Cao, 2009). During the summer, these large reductions in surface J~~which results in higher rates of O^1D ~~and JNO_2 could lead to lower O_3 levels than if particulate levels were low. As demonstrated by Li et al. (2011), the probability of O_3 peaks greater than 120 ppbv increased dramatically with the removal of aerosol from their simulations, and the response of OH concentrations was shown to be approximately linear to changes in JO^1D. Therefore, if controls were implemented to reduce aerosol concentrations, the subsequent increases in JO^1D at the surface could lead to enhanced O_3 concentrations, a major problem in Beijing where summer O_3 is already very high (Wang et al., 2006; Xue et al., 2014; Ni et al., 2018). Enhanced near-surface photolysis rates would also increase O_3 production via NO_2 photolysis, however this would be balanced by the equivalent rise in NO from NO_2 photolysis. Furthermore, the enhancement of JO^1D would increase OH concentrations which would subsequently increase HO_2 and RO_2 and lead to a net rise in O_3 concentrations. In the winter, a similar response would be expected, although due to lower photolysis rates and much lower O_3 concentrations, the effects of particulate control strategies would have a lesser effect on oxidant concentrations.~~ formation (Tie and Cao, 2009), as discussed in Section 4.1.

~~To evaluate the potential photochemical impact on oxidants, a simple experiment was performed using a photochemical box model incorporating the generic reaction set for volatile organic compound oxidation (Topping et al., 2018). The response of O_3 concentrations to the presence of aerosols is similar to that of JO^1D in both seasons with the biggest reductions (12.0 % or larger) seen in the lowest 500 m, see Figure 6. These reductions are more pronounced throughout the day in the winter than in the summer months. The effect of scattering aerosol can be seen further up the column, where enhanced photolysis rates due to aerosol result in increases in O_3 concentrations of 3.0–6.0 %. As with the photolysis rates, the largest impacts are seen in the middle of the day and lower down the column during the summer. The impacts on OH largely match those on O_3, but the responses are much smaller, with 0.0–3.0 % decrease at the surface in winter and a similar magnitude increase higher up the column in the summer.~~

~~The implication of this is that if aerosols were not present surface O_3 and OH concentrations would in fact be higher by around 12.0 % and 3.0 % respectively. In contrast, removal of aerosols would see drops in O_3 higher up the column, particularly in the summer due to the removal of scattering aerosol and the resultant reductions in JO^1D and JNO_2 (see above). In the winter, when O_3 are much lower this may have little impact, but during the summer months when daytime concentrations can exceed 100 ppbv, this could see a potential shift towards more frequent O_3 pollution episodes. It should be noted here however, that in this idealised box model scheme, the photolysis of HONO is not included. HONO photolysis occurs as similar wavelengths to that of NO_2 and is an important source of OH in urban environments. Therefore chemical impacts simulated here, particularly~~

~~for OH, may be underestimated. Therefore, a much more detailed treatment of gas-phase and heterogeneous chemistry in a box model or regional air quality model is needed to fully quantify the impact of these photolysis rate changes on urban oxidant concentrations under haze conditions.~~

The diurnal pattern of haze impacts on photolysis is shown to differ between winter and summer (Figure 4) with the reductions in $J[O^1D]$ and $J[NO_2]$ extending further up through the column during winter. This reflects the much deeper haze layers at the surface throughout the winter (Figure 2). In the summer months, during the middle part of the day, significant reductions in photolysis occur near the surface but at higher altitudes aerosols result in increases of between ~~6.0 and 16.0~~6 and 16 % depending on the species. Therefore, any reductions in aerosol concentrations during the summer months and thus reduction in this scattering effect (particularly from OA), would reduce $J[O^1D]$ and $J[NO_2]$ higher up in the column. As discussed above, lower values of $J[O^1D]$ and $J[NO_2]$ could reduce O_3 and OH concentrations, and thus potentially have important implications for the oxidation capacity in the free troposphere.

Previous work has shown that in air masses influenced by urban pollution, the impacts of aerosol on photolysis rates are greater than the influence of cloud cover (Tang et al., 2003). This study shows that during moderate to severe haze events in Beijing, which occur in both summer and winter, the response of photolysis to aerosol often dominates over cloud~~with contrasting results~~. In the winter absorbing aerosol dominates over cloud at the surface leading to 28.5–30.9 % reductions in photolysis rates compared to just 6.6–7.4 % reductions from the presence of clouds. In the summer, cloud impacts dominate near the surface with the scattering effect from an elevated layer of predominantly OA (Figure 2) taking over at around 3–4 km altitude where photolysis rates are increased by 12.0–13.7 % compared to very minor decreases from cloud (0.24–0.32 %). These patterns are in agreement with previous studies which also demonstrate dominant responses to aerosol in urban air plumes (Liao et al., 1999; Tang et al., 2003). In addition, this work agrees with that of Liao et al. (1999) that the presence of a cloud layer acts to accentuate the reduction in surface photolysis rates for the two reactions considered here. Furthermore, in winter in particular, for the average impacts over all days in the campaign period, the aerosol effects (15.9–17.3 % reductions) are roughly double the cloud impacts (7.9–8.1 % reductions) in the surface layer. This highlights despite the very episodic nature of haze events in Beijing (Figure 1), background aerosol concentrations are still sufficiently high enough at the surface to produce significant reductions in photolysis rate constants. This is likely due to reasonably high AOD values attributed to BC and $(NH_4)_2SO_4$ on the cleaner days (Figure 2). It should be noted that this response is representative for the APHH winter campaign only and these respective effects of cloud and aerosol species are likely to vary greatly between different winter seasons. The results presented in this study however emphasise the significant impact particulate pollution can have on photochemistry.

The results presented here are at the lower end of previous estimates on the impacts of aerosol on photolysis rates (Liao et al., 1999; Tang et al., 2003; Li et al., 2011). For example, Tang et al. (2003) estimate 29.2–38.5 % reductions in $J[O^1D]$ in the lowest 3 km whereas Li et al. (2011) present reductions of 37.2–53.3 %. This study estimates 5.4–30.8 % reductions in the winter and 6.1 % reductions to 8.8 % increases in the lowest 3 km in the summer. These studies either use limited aircraft data AOD (Tang et al., 2003) or total column AOD data (from a combination of satellite and ground based instruments (Li et al., 2011)) to verify the aerosol fields and thus were unable to fully verify the accuracy of the vertical distributions of different

aerosol species throughout the column. The results presented in this work greatly extend these earlier estimates by using a combined statistical and observation driven approach to derive chemically apportioned aerosol extinction from lidar data. This allows more accurate constraint of the vertical distribution of aerosol to be made, including which species provide the largest contribution to extinction throughout the column. As discussed above, this results in layers of haze near to the surface (≈3 km in winter and ≈1 km in summer) dominated by absorbing species in the winter (BC) and scattering species in the summer (OA). This leads to large reductions in $J[O^1D]$ and $J[NO_2]$ at the surface and significant increases at altitude during both campaigns. These increases at height are more emphasised during the summer due to the backscatter from the layer of OA present at the surface (Figure 2). This accounts for the difference in patterns observed between this study and the previous estimates by Tang et al. (2003); Li et al. (2011) and highlights the sensitivity of the responses in photolysis rates not only to the vertical distribution of aerosol but also the chemical speciation of the particulates. The observation constrained approach presented here provides the best possible estimate of both allowing more accurate quantification of the impacts of haze pollution on photolysis rates. Running the Fast-JX code in 'offline' mode also enables the relative impacts of clouds and different aerosol species to be quantified independently. This allows a critical evaluation of whether clouds or a particular aerosol species is causing the greatest photochemical impact during a specific pollution episode to gain insight as where to target particulate matter control strategies.

4.1 Potential photochemical impacts of haze pollution and implications for pollution control strategies

The large reductions in surface $J[O^1D]$ and $J[NO_2]$ during haze events could however be contributing to lower O_3 than if aerosol loadings were low, particularly in the summer months. Therefore removal aerosols alone could potentially enhance surface O_3 pollution. As demonstrated by Li et al. (2011), the probability of O_3 peaks greater than 120 ppbv increased dramatically with the removal of aerosol from their simulations, and the response of OH concentrations was shown to be approximately linear to changes in $J[O^1D]$. Therefore, under the recent reductions in $PM_{2.5}$ in Beijing through emissions controls implemented as part of China's clean air plans (Wang et al., 2015; Liu et al., 2016), the resultant increases in $J[O^1D]$ could potentially lead to enhanced O_3 concentrations, where summer levels are already very high (Wang et al., 2006; Xue et al., 2014; Ni et al., 2018). Enhanced near-surface photolysis rates would also increase O_3 production via NO_2 photolysis and enhanced levels of NO. This rise in O_3 will be partially balanced by the reaction of NO with O_3 itself. However, higher NO levels will also contribute to enhanced O_3 formation through increases in RO_2 and NO reactions. Furthermore, the enhancement of $J[O^1D]$ would increase OH concentrations which would subsequently increase HO_2 and RO_2 and lead to a net rise in O_3 concentrations. In the winter, a similar response would be expected, although due to lower photolysis rates and much lower O_3 concentrations, the effects of particulate control strategies would have a lesser effect on oxidant concentrations.

To evaluate the potential photochemical impact on oxidants, a simple experiment was performed using a photochemical box model incorporating the generic reaction set for volatile organic compound oxidation (Topping et al., 2018). The response of O_3 concentrations to the presence of aerosols is similar to that of $J[O^1D]$ in both seasons with the biggest reductions (12 % or larger) seen in the lowest 500 m, see Figure 6. These reductions are more pronounced throughout the day in the winter than in the summer months. The effect of scattering aerosol can be seen further up the column, where enhanced photolysis rates

due to aerosol result in increases in O_3 concentrations of 3–6 %. As with the photolysis rates, the largest impacts are seen in the middle of the day and lower down the column during the summer. The impacts on OH largely match those on O_3, but the responses are much smaller, with 0–3 % decrease at the surface in winter and a similar magnitude increase higher up the column in the summer.

The implication of this is that if aerosols were not present surface O_3 and OH concentrations would in fact be higher by around 12 % and 3 % respectively. In contrast, removal of aerosols would see drops in O_3 higher up the column, particularly in the summer due to the removal of scattering aerosol and the resultant reductions in J[O^1D] and J[NO_2] (see above). In the winter, when O_3 are much lower this may have little impact, but during the summer months when daytime concentrations can exceed 100 ppbv, this could see a potential shift towards more frequent O_3 pollution episodes. It should be noted here however, that in this idealised box model scheme, the photolysis of HONO is not included. HONO photolysis occurs as similar wavelengths to that of NO_2 and is an important source of OH in urban environments. Therefore chemical impacts simulated here, particularly for OH, may be underestimated. Therefore, a much more detailed treatment of gas-phase and heteorogeneous chemistry in a box model or regional air quality model is needed to fully quantify the impact of these photolysis rate changes on urban oxidant concentrations under haze conditions.

5 Conclusions

This study presents, for the first time, application of aerosol composition data and lidar extinction profiles to drive the Fast-JX photolysis model in order to quantify the effects of severe haze pollution on J[O^1D] and J[NO_2] over Beijing during two intensive measurement campaign periods (winter 2016 and summer 2017). The model is shown to capture observed J[O^1D] and J[NO_2] well during both campaigns, particularly the reductions that occur during haze events (AQI > 100). Such episodes occur during both campaign periods and lead to reductions in surface J[O^1D] of ~~27.4~~27 % (summer) to ~~33.7~~34 % (winter) and reductions of ~~40.4~~40 % (winter) to ~~66.2~~66 % (summer) in J[NO_2]. Despite much lower particulate concentrations in the summer campaign, the absolute changes in photolysis rates are shown to be larger than in winter for both O_3 and NO_2.

In the winter, absorbing aerosols such as BC are shown to dominate the photolysis response to aerosol leading to mean reductions of 23.8 % and 23.1 % respectively for J[O^1D] and J[NO_2] in the lowest 1 km. In contrast, in the summer, scattering aerosols such as OA dominate the response leading to mean decreases of around ~~2.4–3.8~~2–4 % at the surface and increases of ~~8.4–10.1~~8–10 % at higher altitudes (3–4 km). During haze episodes, these effects often dominate over those attributed to cloud cover. This emphasises that in heavily polluted urban environments such as Beijing, aerosols are present in such large concentrations that they produce larger impacts on photolysis than naturally occurring phenomena such as clouds, and are likely to have other important chemical and dynamical impacts on the urban environment.

The ~~results presented here greatly improve on previous studies by using a combined statistical and observational driven approach to provide a more accurate representation of the vertical distribution and speciation of aerosol extinction. This~~ observation-driven approach to deriving the aerosol vertical distribution allows a more accurate constraint to be made on the estimated impacts of haze pollution on photochemistry ~~. Critically, this shows which aerosol species is causing the largest~~

~~photochemical impact during each campaign period and therefore allowing the identification of which~~ and, more critically, allows species specific impacts to be highlighted. This allows the potential identification of source sectors to target particulate control strategies on. For example during the APHH winter campaign, sources of BC (e.g. power generation, residential heating) contribute the most to photochemical impacts during haze events. Such strategies would not only reduce ~~pollutant concentrationsbut would also offset the photochemical impacts demonstrated here~~particulate matter concentrations, but also reduce their impacts on photolysis rates and thus potentially increase surface ozone concentrations. Furthermore, the non local impact of potential emissions and pollution control strategies is emphasised. Emissions cuts implemented at the surface not only produce large impacts in surface oxidant concentrations but also result in significant impacts in the free troposphere.

Using an idealised photochemical box model, if particulates were completely removed during the APHH campaigns, surface O_3 concentrations could be enhanced by around ~~12.0~~12 % (~~3.0~~3 % for OH). In contrast, particulate controls could reduce O_3 by ~~3.0–6.0~~3–6 % in the free troposphere. However, any control policy is also likely to impact concentrations of other pollutants such as NO_x and VOCs and therefore due to the complex non-linearities involved, the response of atmospheric oxidants is likely to vary dependent on the magnitudes of the emissions changes. To fully quantify the effects of pollutant haze on the urban atmospheric oxidation capacity, a more detailed air quality model study is needed that fully incorporates the optical properties of urban aerosol and their impacts on photolysis rates demonstrated here along with treatment of gas-phase and heterogeneous photochemistry and urban meteorology.

Data availability. The data generated in this study will be made available through the CEDA data archive at (details released on publication). The processed single particle soot photometer (SP2) data used in this study are available through the CEDA data archive (https://catalogue.ceda.ac.uk/uuid/a The processed photolysis observations used in this study are available through the CEDA archive (https://catalogue.ceda.ac.uk/uuid/76b4ad364d71465d8f8

Author contributions. MH and OW conceived this study. MH performed the data analysis and ran model simulations. TY collected and provided the lidar data at the IAP tower site. YS, WX and CX collected and provided the aerosol composition data and optical properties measured at the tower site. LW, ES and DH collected and provided the observed photolysis rates. DL collected and provided the optical properties for black carbon from the SP2 instrument. MH and OW wrote the manuscript with input from all authors.

Competing interests. The authors declare that they have no conflict of interest.

Acknowledgements. This authors acknowledge funding from the AIRPRO (An Integrated Study of Air Pollution PROcesses in Beijing) project, a Newton Innovation Fund project funded by the UK Natural Environment Research Council (Grant Numbers NE/N006925/1, NE/N006895/1 and NE/N007123/1), the Strategic Priority Research Program of the Chinese Academy of Sciences 'Beautiful China' project

(Grant Number XDA19040203) and the Natural Science Foundation of China (Grant Number 41571130034). ES acknowledges funding from the SPHERES NERC Doctoral Training Programme.

References

Bian, H. and Prather, M. J.: Fast-J2: Accurate Simulation of Stratospheric Photolysis in Global Chemical Models, Journal of Atmospheric Chemistry, 41, 281–296, https://doi.org/10.1023/A:1014980619462, 2002.

Bian, H., Prather, M. J., and Takemura, T.: Tropospheric aerosol impacts on trace gas budgets through photolysis, Journal of Geophysical Research: Atmospheres, 108, https://doi.org/10.1029/2002JD002743, 2003.

CAMS: CAMS Reanalysis data documentation. Copernicus Atmosphere Modelling Service (CAMS), https://confluence.ecmwf.int/display/CKB/CAMS+Reanalysis+data+documentation, last access: 2018-08-16, 2018.

Chan, C. K. and Yao, X.: Air pollution in mega cities in China, Atmospheric Environment, 42, 1 – 42, https://doi.org/10.1016/j.atmosenv.2007.09.003, 2008.

Chen, Y., Zhao, C., Zhang, Q., Deng, Z., Huang, M., and Ma, X.: Aircraft study of Mountain Chimney Effect of Beijing, China, Journal of Geophysical Research: Atmospheres, 114, https://doi.org/10.1029/2008JD010610, 2009.

Cheng, S. H., Yang, L. X., Zhou, X. H., Xue, L. K., Gao, X. M., Zhou, Y., and Wang, W. X.: Size-fractionated water-soluble ions, situ pH and water content in aerosol on hazy days and the influences on visibility impairment in Jinan, China, Atmospheric Environment, 45, 4631 – 4640, https://doi.org/https://doi.org/10.1016/j.atmosenv.2011.05.057, 2011.

DeCarlo, P. F., Kimmel, J. R., Trimborn, A., Northway, M. J., Jayne, J. T., Aiken, A. C., Gonin, M., Fuhrer, K., Horvath, T., Docherty, K. S., Worsnop, D. R., and Jimenez, J. L.: Field-Deployable, High-Resolution, Time-of-Flight Aerosol Mass Spectrometer, Analytical Chemistry, 78, 8281–8289, https://doi.org/10.1021/ac061249n, pMID: 17165817, 2006.

Drinovec, L., Močnik, G., Zotter, P., Prévôt, A. S. H., Ruckstuhl, C., Coz, E., Rupakheti, M., Sciare, J., Müller, T., Wiedensohler, A., and Hansen, A. D. A.: The "dual-spot" Aethalometer: an improved measurement of aerosol black carbon with real-time loading compensation, Atmospheric Measurement Techniques, 8, 1965–1979, https://doi.org/10.5194/amt-8-1965-2015, 2015.

ECMWF: ERA5 data documentation. European Centre for Medium-range Weather Forecast (ECMWF), https://confluence.ecmwf.int/display/CKB/ERA5+data+documentation, last access: 2018-08-16, 2018.

Hall, S. R., Ullmann, K., Prather, M. J., Flynn, C. M., Murray, L. T., Fiore, A. M., Correa, G., Strode, S. A., Steenrod, S. D., Lamarque, J.-F., Guth, J., Josse, B., Flemming, J., Huijnen, V., Abraham, N. L., and Archibald, A. T.: Cloud impacts on photochemistry: building a climatology of photolysis rates from the Atmospheric Tomography mission, Atmospheric Chemistry and Physics, 18, 16 809–16 828, https://doi.org/10.5194/acp-18-16809-2018, 2018.

Han, T., Xu, W., Chen, C., Liu, X., Wang, Q., Li, J., Zhao, X., Du, W., Wang, Z., and Sun, Y.: Chemical apportionment of aerosol optical properties during the Asia-Pacific Economic Cooperation summit in Beijing, China, Journal of Geophysical Research: Atmospheres, 120, 12,281–12,295, https://doi.org/10.1002/2015JD023918, 2015.

Henyey, L. G. and Greenstein, J. L.: Diffuse radiation in the Galaxy, apj, 93, 70–83, https://doi.org/10.1086/144246, 1941.

Hu, B., Zhao, X., Liu, H., Liu, Z., Song, T., Wang, Y., Tang, L., Xia, X., Tang, G., Ji, D., Wen, T., Wang, L., Sun, Y., and Xin, J.: Quantification of the impact of aerosol on broadband solar radiation in North China, Scientific Reports, 7, 44 851, https://doi.org/10.1038/srep44851, 2017.

Huang, R.-J., Zhang, Y., Bozzetti, C., Ho, K.-F., Cao, J.-J., Han, Y., Daellenbach, K. R., Slowik, J. G., Platt, S. M., Canonaco, F., Zotter, P., Wolf, R., Pieber, S. M., Bruns, E. A., Crippa, M., Ciarelli, G., Piazzalunga, A., Schwikowski, M., Abbaszade, G., Schnelle-Kreis, J., Zimmermann, R., An, Z., Szidat, S., Baltensperger, U., Haddad, I. E., and Prévôt, A. S. H.: High secondary aerosol contribution to particulate pollution during haze events in China, Nature, 514, 218, https://doi.org/10.1038/nature13774, 2014.

Inness, A., Ades, M., Agusti-Panareda, A., Barré, J., Benedictow, A., Blechschmidt, A.-M., Dominguez, J. J., Engelen, R., Eskes, H., Flemming, J., Huijnen, V., Jones, L., Kipling, Z., Massart, S., Parrington, M., Peuch, V.-H., Razinger, M., Remy, S., Schulz, M., and Suttie, M.: The CAMS reanalysis of atmospheric composition, Atmospheric Chemistry and Physics Discussions, 2018, 1–55, https://doi.org/10.5194/acp-2018-1078, https://www.atmos-chem-phys-discuss.net/acp-2018-1078/, 2018.

Ji, D., Li, L., Wang, Y., Zhang, J., Cheng, M., Sun, Y., Liu, Z., Wang, L., Tang, G., Hu, B., Chao, N., Wen, T., and Miao, H.: The heaviest particulate air-pollution episodes occurred in northern China in January, 2013: Insights gained from observation, Atmospheric Environment, 92, 546 – 556, https://doi.org/https://doi.org/10.1016/j.atmosenv.2014.04.048, 2014.

Kaiser, D. P. and Qian, Y.: Decreasing trends in sunshine duration over China for 1954–1998: Indication of increased haze pollution?, Geophysical Research Letters, 29, 38–1–38–4, https://doi.org/10.1029/2002GL016057, 2002.

Lelieveld, J., Evans, J. S., Fnais, M., Giannadaki, D., and Pozzer, A.: The contribution of outdoor air pollution sources to premature mortality on a global scale, Nature, 525, 367–371, https://doi.org/10.1038/nature15371, 2015.

Li, G., Zhang, R., Fan, J., and Tie, X.: Impacts of black carbon aerosol on photolysis and ozone, Journal of Geophysical Research: Atmospheres, 110, https://doi.org/10.1029/2005JD005898, 2005.

Li, J., Wang, Z., Wang, X., Yamaji, K., Takigawa, M., Kanaya, Y., Pochanart, P., Liu, Y., Irie, H., Hu, B., Tanimoto, H., and Akimoto, H.: Impacts of aerosols on summertime tropospheric photolysis frequencies and photochemistry over Central Eastern China, Atmospheric Environment, 45, 1817 – 1829, https://doi.org/https://doi.org/10.1016/j.atmosenv.2011.01.016, 2011.

Li, J., Fu, Q., Huo, J., Wang, D., Yang, W., Bian, Q., Duan, Y., Zhang, Y., Pan, J., Lin, Y., Huang, K., Bai, Z., Wang, S.-H., Fu, J. S., and Louie, P. K.: Tethered balloon-based black carbon profiles within the lower troposphere of Shanghai in the 2013 East China smog, Atmospheric Environment, 123, 327 – 338, https://doi.org/https://doi.org/10.1016/j.atmosenv.2015.08.096, 2015.

Liao, H., Yung, Y. L., and Seinfeld, J. H.: Effects of aerosols on tropospheric photolysis rates in clear and cloudy atmospheres, Journal of Geophysical Research: Atmospheres, 104, 23 697–23 707, https://doi.org/10.1029/1999JD900409, 1999.

Liu, D., Flynn, M., Gysel, M., Targino, A., Crawford, I., Bower, K., Choularton, T., Jurányi, Z., Steinbacher, M., Hüglin, C., Curtius, J., Kampus, M., Petzold, A., Weingartner, E., Baltensperger, U., and Coe, H.: Single particle characterization of black carbon aerosols at a tropospheric alpine site in Switzerland, Atmospheric Chemistry and Physics, 10, 7389–7407, https://doi.org/10.5194/acp-10-7389-2010, 2010.

Liu, D., Allan, J. D., Young, D. E., Coe, H., Beddows, D., Fleming, Z. L., Flynn, M. J., Gallagher, M. W., Harrison, R. M., Lee, J., Prevot, A. S. H., Taylor, J. W., Yin, J., Williams, P. I., and Zotter, P.: Size distribution, mixing state and source apportionment of black carbon aerosol in London during wintertime, Atmospheric Chemistry and Physics, 14, 10 061–10 084, https://doi.org/10.5194/acp-14-10061-2014, 2014.

Liu, D., Joshi, R., Wang, J., Yu, C., Allan, J. D., Coe, H., Flynn, M. J., Xie, C., Lee, J., Squires, F., Kotthaus, S., Grimmond, S., Ge, X., Sun, Y., and Fu, P.: Contrasting physical properties of black carbon in urban Beijing between winter and summer, Atmospheric Chemistry and Physics Discussions, 2018, 1–30, https://doi.org/10.5194/acp-2018-1142, https://www.atmos-chem-phys-discuss.net/acp-2018-1142/, 2018a.

Liu, F., Zhang, Q., van der A, R. J., Zheng, B., Tong, D., Yan, L., Zheng, Y., and He, K.: Recent reduction in NO x emissions over China: synthesis of satellite observations and emission inventories, Environmental Research Letters, 11, 114 002, https://doi.org/10.1088/1748-9326/11/11/114002, 2016.

Liu, Q., Ding, D., Huang, M., Tian, P., Zhao, D., Wang, F., Li, X., Bi, K., Sheng, J., Zhou, W., Liu, D., Huang, R., and Zhao, C.: A study of elevated pollution layer over the North China Plain using aircraft measurements, Atmospheric Environment, 190, 188 – 194,

https://doi.org/https://doi.org/10.1016/j.atmosenv.2018.07.024, http://www.sciencedirect.com/science/article/pii/S1352231018304710, 2018b.

Lou, S., Liao, H., and Zhu, B.: Impacts of aerosols on surface-layer ozone concentrations in China through heterogeneous reactions and changes in photolysis rates, Atmospheric Environment, 85, 123 – 138, https://doi.org/https://doi.org/10.1016/j.atmosenv.2013.12.004, 2014.

Martin, R. V., Jacob, D. J., Yantosca, R. M., Chin, M., and Ginoux, P.: Global and regional decreases in tropospheric oxidants from photochemical effects of aerosols, Journal of Geophysical Research: Atmospheres, 108, https://doi.org/10.1029/2002JD002622, 2003.

Mentel, T. F., Kleist, E., Andres, S., Dal Maso, M., Hohaus, T., Kiendler-Scharr, A., Rudich, Y., Springer, M., Tillmann, R., Uerlings, R., Wahner, A., and Wildt, J.: Secondary aerosol formation from stress-induced biogenic emissions and possible climate feedbacks, Atmospheric Chemistry and Physics, 13, 8755–8770, https://doi.org/10.5194/acp-13-8755-2013, 2013.

Neu, J. L., Prather, M. J., and Penner, J. E.: Global atmospheric chemistry: Integrating over fractional cloud cover, Journal of Geophysical Research: Atmospheres, 112, https://doi.org/10.1029/2006JD008007, 2007.

Ni, R., Lin, J., Yan, Y., and Lin, W.: Foreign and domestic contributions to springtime ozone over China, Atmospheric Chemistry and Physics, 18, 11 447–11 469, https://doi.org/10.5194/acp-18-11447-2018, 2018.

Pitchford, M., Malm, W., Schichtel, B., Kumar, N., Lowenthal, D., and Hand, J.: Revised Algorithm for Estimating Light Extinction from IMPROVE Particle Speciation Data, Journal of the Air & Waste Management Association, 57, 1326–1336, https://doi.org/10.3155/1047-3289.57.11.1326, 2007.

Prather, M. J.: Photolysis rates in correlated overlapping cloud fields: Cloud-J 7.3c, Geoscientific Model Development, 8, 2587–2595, https://doi.org/10.5194/gmd-8-2587-2015, 2015.

Ran, L., Deng, Z., Xu, X., Yan, P., Lin, W., Wang, Y., Tian, P., Wang, P., Pan, W., and Lu, D.: Vertical profiles of black carbon measured by a micro-aethalometer in summer in the North China Plain, Atmospheric Chemistry and Physics, 16, 10 441–10 454, https://doi.org/10.5194/acp-16-10441-2016, 2016.

Riipinen, I., Pierce, J. R., Yli-Juuti, T., Nieminen, T., Häkkinen, S., Ehn, M., Junninen, H., Lehtipalo, K., Petäjä, T., Slowik, J., Chang, R., Shantz, N. C., Abbatt, J., Leaitch, W. R., Kerminen, V.-M., Worsnop, D. R., Pandis, S. N., Donahue, N. M., and Kulmala, M.: Organic condensation: a vital link connecting aerosol formation to cloud condensation nuclei (CCN) concentrations, Atmospheric Chemistry and Physics, 11, 3865–3878, https://doi.org/10.5194/acp-11-3865-2011, 2011.

Shen, G., Xue, M., Yuan, S., Zhang, J., Zhao, Q., Li, B., Wu, H., and Ding, A.: Chemical compositions and reconstructed light extinction coefficients of particulate matter in a mega-city in the western Yangtze River Delta, China, Atmospheric Environment, 83, 14 – 20, https://doi.org/https://doi.org/10.1016/j.atmosenv.2013.10.055, 2014.

Shi, Z., Vu, T., Kotthaus, S., Harrison, R. M., Grimmond, S., Yue, S., Zhu, T., Lee, J., Han, Y., Demuzere, M., Dunmore, R. E., Ren, L., Liu, D., Wang, Y., Wild, O., Allan, J., Acton, W. J., Barlow, J., Barratt, B., Beddows, D., Bloss, W. J., Calzolai, G., Carruthers, D., Carslaw, D. C., Chan, Q., Chatzidiakou, L., Chen, Y., Crilley, L., Coe, H., Dai, T., Doherty, R., Duan, F., Fu, P., Ge, B., Ge, M., Guan, D., Hamilton, J. F., He, K., Heal, M., Heard, D., Hewitt, C. N., Hollaway, M., Hu, M., Ji, D., Jiang, X., Jones, R., Kalberer, M., Kelly, F. J., Kramer, L., Langford, B., Lin, C., Lewis, A. C., Li, J., Li, W., Liu, H., Liu, J., Loh, M., Lu, K., Lucarelli, F., Mann, G., McFiggans, G., Miller, M. R., Mills, G., Monk, P., Nemitz, E., O'Connor, F., Ouyang, B., Palmer, P. I., Percival, C., Popoola, O., Reeves, C., Rickard, A. R., Shao, L., Shi, G., Spracklen, D., Stevenson, D., Sun, Y., Sun, Z., Tao, S., Tong, S., Wang, Q., Wang, W., Wang, X., Wang, X., Wang, Z., Wei, L., Whalley, L., Wu, X., Wu, Z., Xie, P., Yang, F., Zhang, Q., Zhang, Y., Zhang, Y., and Zheng, M.: Introduction to the special issue "In-depth

study of air pollution sources and processes within Beijing and its surrounding region (APHH-Beijing)", Atmospheric Chemistry and Physics, 19, 7519–7546, https://doi.org/10.5194/acp-19-7519-2019, 2019.

Sugimoto, N., Matsui, I., Shimizu, A., Uno, I., Asai, K., Endoh, T., and Nakajima, T.: Observation of dust and anthropogenic aerosol plumes in the Northwest Pacific with a two-wavelength polarization lidar on board the research vessel Mirai, Geophysical Research Letters, 29, 7–1–7–4, https://doi.org/10.1029/2002GL015112, 2002.

Sun, Y., Song, T., Tang, G., and Wang, Y.: The vertical distribution of PM2.5 and boundary-layer structure during summer haze in Beijing, Atmospheric Environment, 74, 413 – 421, https://doi.org/https://doi.org/10.1016/j.atmosenv.2013.03.011, 2013.

Tang, Y., Carmichael, G. R., Uno, I., Woo, J.-H., Kurata, G., Lefer, B., Shetter, R. E., Huang, H., Anderson, B. E., Avery, M. A., Clarke, A. D., and Blake, D. R.: Impacts of aerosols and clouds on photolysis frequencies and photochemistry during TRACE-P: 2. Three-dimensional study using a regional chemical transport model, Journal of Geophysical Research: Atmospheres, 108, https://doi.org/10.1029/2002JD003100, 2003.

Tie, X. and Cao, J.: Aerosol pollution in China: Present and future impact on environment, Particuology, 7, 426 – 431, https://doi.org/https://doi.org/10.1016/j.partic.2009.09.003, 2009.

Topping, D., Connolly, P., and Reid, J.: PyBox: An automated box-model generator for atmospheric chemistry and aerosol simulations., The Journal of Open Source Software, 3, https://doi.org/https://doi.org/10.21105/joss.00755, 2018.

Wang, L. T., Wei, Z., Yang, J., Zhang, Y., Zhang, F. F., Su, J., Meng, C. C., and Zhang, Q.: The 2013 severe haze over southern Hebei, China: model evaluation, source apportionment, and policy implications, Atmospheric Chemistry and Physics, 14, 3151–3173, https://doi.org/10.5194/acp-14-3151-2014, 2014a.

Wang, Q., Sun, Y., Xu, W., Du, W., Zhou, L., Tang, G., Chen, C., Cheng, X., Zhao, X., Ji, D., Han, T., Wang, Z., Li, J., and Wang, Z.: Vertically resolved characteristics of air pollution during two severe winter haze episodes in urban Beijing, China, Atmospheric Chemistry and Physics, 18, 2495–2509, https://doi.org/10.5194/acp-18-2495-2018, 2018.

Wang, S., Zhang, Q., Martin, R. V., Philip, S., Liu, F., Li, M., Jiang, X., and He, K.: Satellite measurements oversee China's sulfur dioxide emission reductions from coal-fired power plants, Environmental Research Letters, 10, 114 015, https://doi.org/10.1088/1748-9326/10/11/114015, 2015.

Wang, T., Ding, A., Gao, J., and Wu, W. S.: Strong ozone production in urban plumes from Beijing, China, Geophysical Research Letters, 33, https://doi.org/10.1029/2006GL027689, 2006.

Wang, Y., Yao, L., Wang, L., Liu, Z., Ji, D., Tang, G., Zhang, J., Sun, Y., Hu, B., and Xin, J.: Mechanism for the formation of the January 2013 heavy haze pollution episode over central and eastern China, Science China Earth Sciences, 57, 14–25, https://doi.org/10.1007/s11430-013-4773-4, 2014b.

Wang, Z., Li, J., Wang, Z., Yang, W., Tang, X., Ge, B., Yan, P., Zhu, L., Chen, X., Chen, H., Wand, W., Li, J., Liu, B., Wang, X., Wand, W., Zhao, Y., Lu, N., and Su, D.: Modeling study of regional severe hazes over mid-eastern China in January 2013 and its implications on pollution prevention and control, Science China Earth Sciences, 57, 3–13, https://doi.org/10.1007/s11430-013-4793-0, 2014c.

Whalley, L. K., Stone, D., Dunmore, R., Hamilton, J., Hopkins, J. R., Lee, J. D., Lewis, A. C., Williams, P., Kleffmann, J., Laufs, S., Woodward-Massey, R., and Heard, D. E.: Understanding in situ ozone production in the summertime through radical observations and modelling studies during the Clean air for London project (ClearfLo), Atmospheric Chemistry and Physics, 18, 2547–2571, https://doi.org/10.5194/acp-18-2547-2018, https://www.atmos-chem-phys.net/18/2547/2018/, 2018.

Wild, O., Zhu, X., and Prather, M. J.: Fast-J: Accurate Simulation of In- and Below-Cloud Photolysis in Tropospheric Chemical Models, Journal of Atmospheric Chemistry, 37, 245–282, https://doi.org/10.1023/A:1006415919030, 2000.

Xing, J., Wang, J., Mathur, R., Wang, S., Sarwar, G., Pleim, J., Hogrefe, C., Zhang, Y., Jiang, J., Wong, D. C., and Hao, J.: Impacts of aerosol direct effects on tropospheric ozone through changes in atmospheric dynamics and photolysis rates, Atmospheric Chemistry and Physics, 17, 9869–9883, https://doi.org/10.5194/acp-17-9869-2017, 2017.

Xue, L. K., Wang, T., Gao, J., Ding, A. J., Zhou, X. H., Blake, D. R., Wang, X. F., Saunders, S. M., Fan, S. J., Zuo, H. C., Zhang, Q. Z., and Wang, W. X.: Ground-level ozone in four Chinese cities: precursors, regional transport and heterogeneous processes, Atmospheric Chemistry and Physics, 14, 13 175–13 188, https://doi.org/10.5194/acp-14-13175-2014, 2014.

Yang, T., Wang, Z., Zhang, B., Wang, X., Wang, W., Gbauidi, A., and Gong, Y.: Evaluation of the effect of air pollution control during the Beijing 2008 Olympic Games using Lidar data, Chinese Science Bulletin, 55, 1311–1316, https://doi.org/10.1007/s11434-010-0081-y, 2010.

Yang, T., Wang, Z., Zhang, W., Gbaguidi, A., Sugimoto, N., Wang, X., Matsui, I., and Sun, Y.: Technical note: Boundary layer height determination from lidar for improving air pollution episode modeling: development of new algorithm and evaluation, Atmospheric Chemistry and Physics, 17, 6215–6225, https://doi.org/10.5194/acp-17-6215-2017, 2017.

Zhang, Q., Ma, X., Tie, X., Huang, M., and Zhao, C.: Vertical distributions of aerosols under different weather conditions: Analysis of in-situ aircraft measurements in Beijing, China, Atmospheric Environment, 43, 5526 – 5535, https://doi.org/https://doi.org/10.1016/j.atmosenv.2009.05.037, 2009.

Zhang, R., Wang, G., Guo, S., Zamora, M. L., Ying, Q., Lin, Y., Wang, W., Hu, M., and Wang, Y.: Formation of Urban Fine Particulate Matter, Chemical Reviews, 115, 3803–3855, https://doi.org/10.1021/acs.chemrev.5b00067, pMID: 25942499, 2015.

Zhao, X. J., Zhao, P. S., Xu, J., Meng, W., Pu, W. W., Dong, F., He, D., and Shi, Q. F.: Analysis of a winter regional haze event and its formation mechanism in the North China Plain, Atmospheric Chemistry and Physics, 13, 5685–5696, https://doi.org/10.5194/acp-13-5685-2013, 2013.

Zheng, B., Zhang, Q., Zhang, Y., He, K. B., Wang, K., Zheng, G. J., Duan, F. K., Ma, Y. L., and Kimoto, T.: Heterogeneous chemistry: a mechanism missing in current models to explain secondary inorganic aerosol formation during the January 2013 haze episode in North China, Atmospheric Chemistry and Physics, 15, 2031–2049, https://doi.org/10.5194/acp-15-2031-2015, 2015.

Table 1. Model scenarios run during both campaign periods. The column headers indicate whether the radiative effects of each aerosol species/cloud is turned on in the respective scenario

Scenario	Cloud	Aerosol (all)	SO_4^{2-}	NO_3^-	Cl^-	OA	BC
Clear Sky	Off	Off	Off	Off	Off	Off	Off
Cloud Only	**On**	Off	Off	Off	Off	Off	Off
Aerosol Only	Off	**On**	**On**	**On**	**On**	**On**	**On**
SO4 Only	Off	Off	**On**	Off	Off	Off	Off
NO3 Only	Off	Off	Off	**On**	Off	Off	Off
CHL Only	Off	Off	Off	Off	**On**	Off	Off
ORG Only	Off	Off	Off	Off	Off	**On**	Off
BC Only	Off	Off	Off	Off	Off	Off	**On**
Aerosol + Cloud	**On**	**On**	**On**	**On**	**On**	**On**	**On**

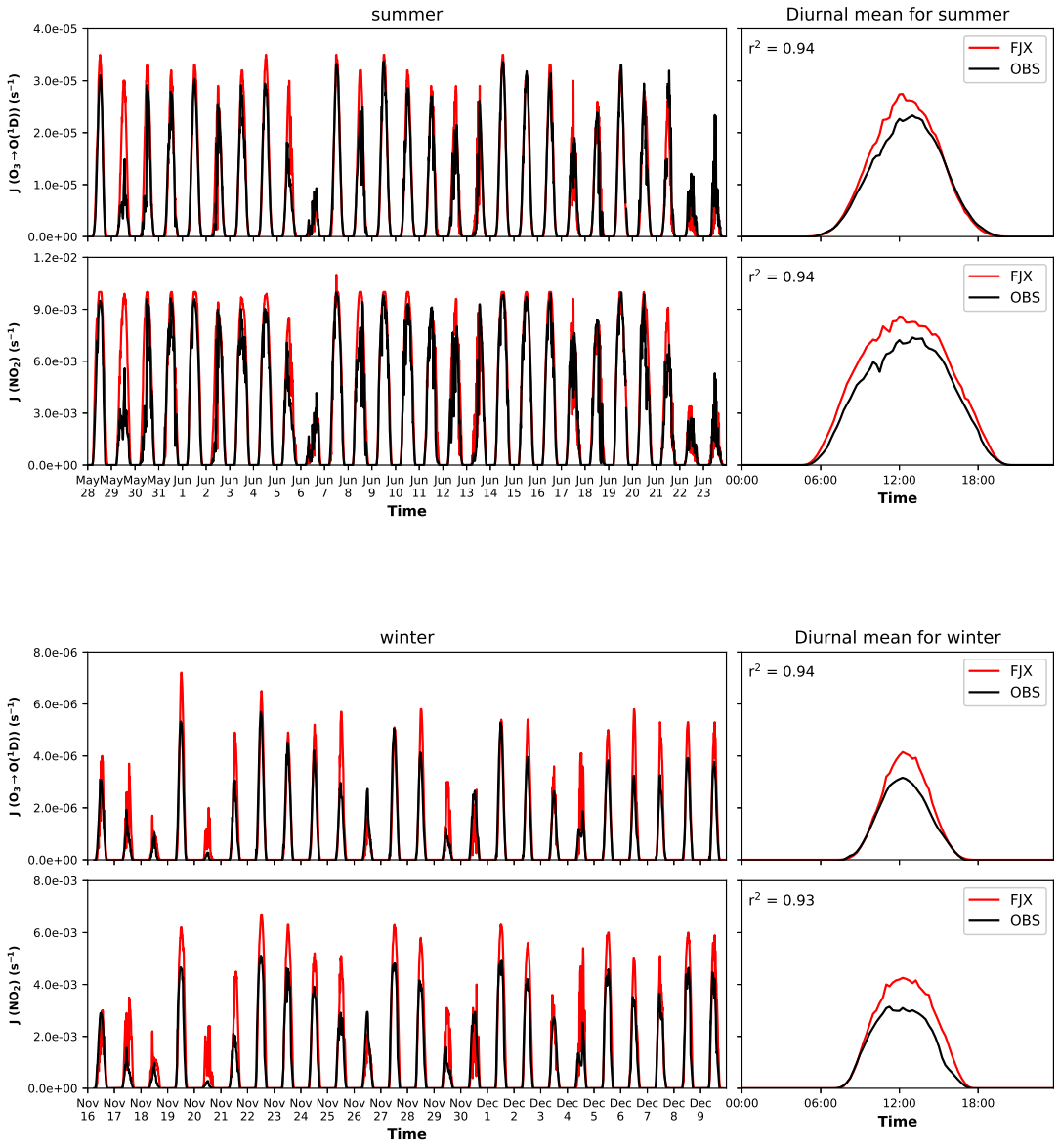

Figure 1. Modelled versus observed photolysis rate constants for the winter (top panel) and summer (bottom panel) campaign periods. Time series (left hand plots) and campaign diurnal averages (right hand plots) of J[O^1D] and J[NO_2] are shown for simulations with Fast-JX (FJX) including cloud and aerosol (red lines) and for observations. Note the difference in magnitude of rate constants between summer and winter. The r^2 value for model versus observed hourly photolysis rates are shown in the right hand plots for reference.

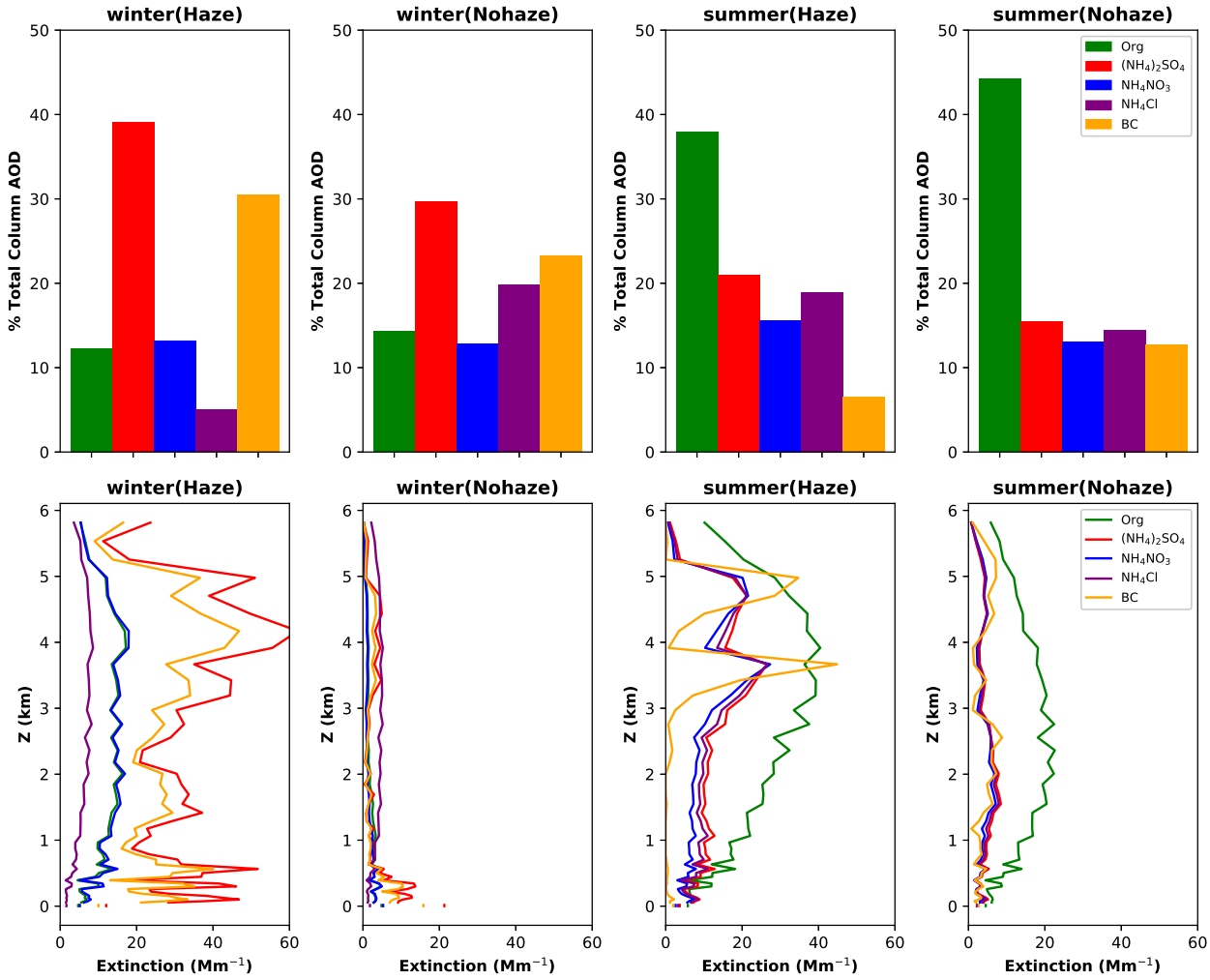

Figure 2. Contributions to total column AOD (top plots) and vertical profiles of ~~AOD~~ extinction (lower plots) for each aerosol component as derived from the optimisation approach. Data are presented for for haze and non-haze periods (see text for definition) in both campaigns from the surface up to 6 km altitude.

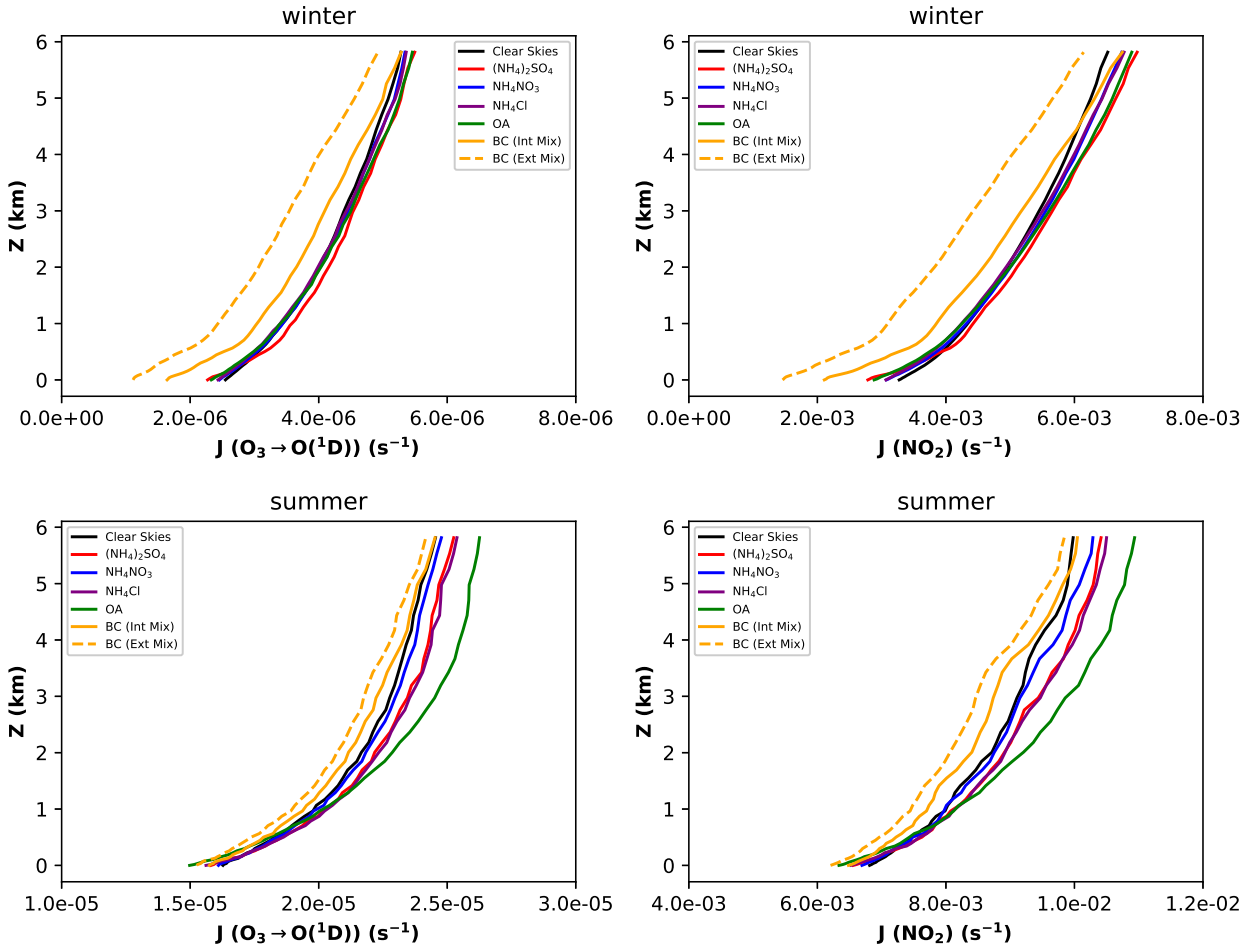

Figure 3. Vertical profiles of J[O^1D] (left) and J[NO_2] (right) for simulations where the radiative effects of each aerosol component is included in isolation. Profiles are shown for the winter (top) and summer campaigns (bottom) and show impacts of OA (solid green), $(NH_4)_2SO_4$ (solid red), NH_4NO_3 (solid blue), NH_4Cl (solid purple) and coated BC (solid orange) and respectively. Photolysis rate constants under clear sky conditions (solid black line) are shown for reference. The radiative impacts of BC when it is assumed to be externally mixed rather than coated is shown for comparison (dashed orange line).

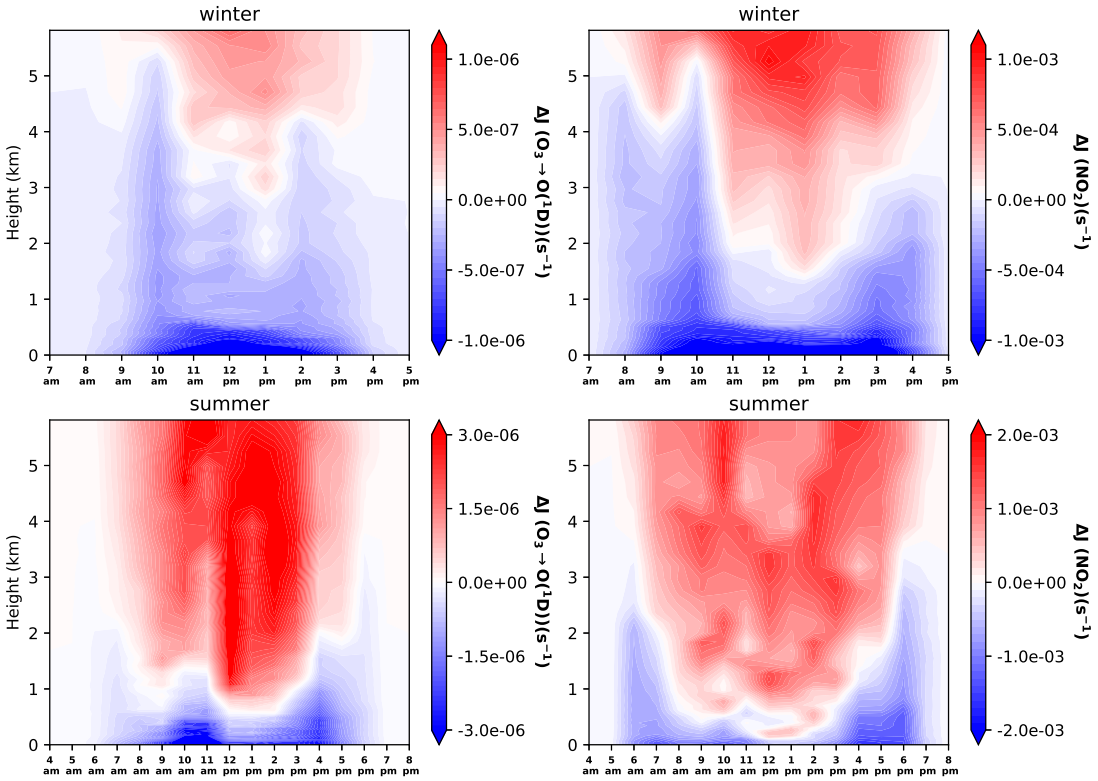

Figure 4. Diurnal profiles of aerosol impacts on J[O^1D] (left column) and J[NO_2] (right column) for winter (top row) and summer (bottom row) campaign periods. Plots show the mean ~~relative~~ absolute difference with respect to clear sky conditions, with blue representing a reduction due to aerosols and red representing an increase. Note the difference in time scales between seasons which reflects longer daylight hours in summer.

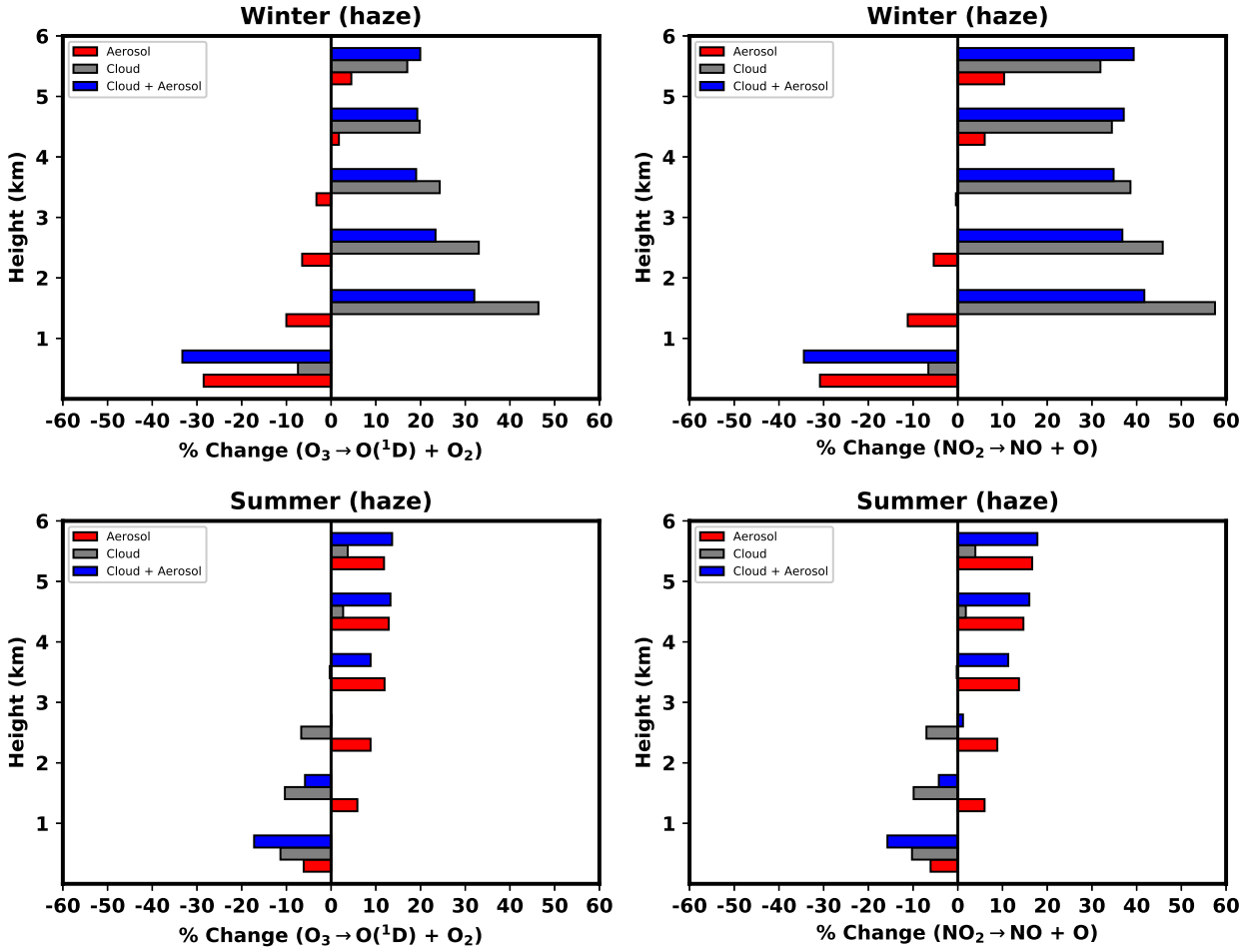

Figure 5. Mean relative impacts of aerosols (red bars), clouds (grey bars) and combined cloud and aerosol (blue bars) on J[O^1D] (left column) and J[NO_2] (right column) during the winter (top row) and summer (bottom row) campaign periods. The relative differences are with respect to clear sky conditions and are calculated as the average for periods classified as haze, in 1 km layers from the surface to 6 km.

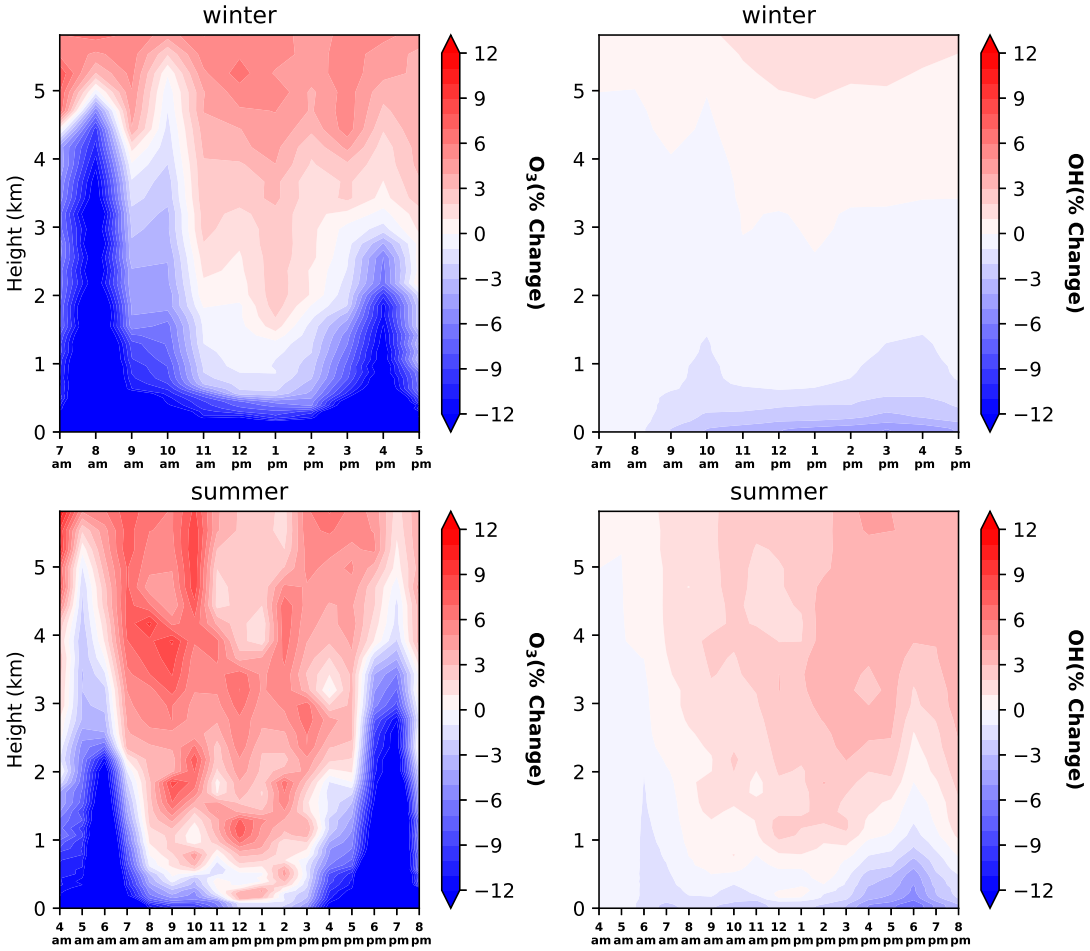

Figure 6. Diurnal profiles of aerosol impacts on O_3 (left column) and OH (right column) concentrations for winter (top row) and summer (bottom row) campaign periods. These changes are calculated using a simple chemical box model, and plots show the mean relative difference with respect to clear sky conditions, with blue representing a reduction due to aerosols and red representing an increase.